ARCADA

DYNAMIC SHEAR MODULUS MEASUREMENT OF THIN PLATES USING TORSIONAL PENDULUM

Name: Saara Ishfaq

DEGREE THESIS	
Arcada	
Degree Programme:	Materials Processing Technology
Identification number:	20783
Author:	Saara Ishfaq
Title:	Dynamic shear modulus measurement of thin plates using torsional pendulum
Supervisor (Arcada):	Rene Herrmann
Examiner:	Mathew Vihtonen

Abstract:

Material testing is an essential step in the product development as it determines the quality and lifetime estimation of a product. The shear test is conducted to determine the behavior of a material under shear strain. This thesis aims to determine the dynamic shear modulus of fixed-fixed thin plates using a torsional pendulum. Torsion test is chosen to be a better alternative than tensile and four-point shear test to obtain the shear properties because it causes only shear stresses and provides purer form of shear in the material. Experimentally, torsional pendulum is used to find the dynamic shear modulus.

The calculation of dynamic shear modulus is based on the standard ASTM E1876-15. The boundary condition of this standard ASTM E1876-15 is free – free. Whereas, this thesis uses fixed-fixed boundary condition. The test specimen is clamped on both ends to suppress other modes of vibration that are existing simultaneously.

The standard ASTM E1876-15 is used to determine the dynamic shear modulus of high-density materials. Whereas, this thesis shows a method to obtain the dynamic shear modulus for light-weight materials. It involves a double clamped torsional pendulum with two equal springs operating in parallel. It is assumed that the coupling of these springs is larger than 2, due to simultaneous contraction while twisting. The coupling parameter is $z(L/w)$ and established using FEA analysis. It is approximately 2.108. The shear modulus calculated using the frequency obtained from COMSOL Multiphysics showed 95% agreement to the tabulated shear modulus of that material. The constructed device showed agreement within 97% of the FEA predicted shear modulus. Experiments were limited to the material with length to width ratio of more than 20 and width to thickness ratio of more than 5 as for larger torsion constants the instrument's frame deforms as well, making frequency measurements inaccurate.

The fundamental difference between the method developed in this thesis and the method of the standard ASTM E1876-15 is that the standard uses a spring with distributed mass only, whereas this thesis uses purposely an external inertia. This results in slower vibrations and consequently smaller measurement errors due to viscous damping. This leads to an improvement compared to the standard ASTM E1876-15.

Keywords:	Dynamic shear modulus, ASTM E1876-15, Torsional pendulum, Non-destructive testing, Finite Element Analysis, Coupling parameter
Number of pages:	82
Language:	English

Contents

4

Figures

Tables

Abbreviations and Units

TERM	DEFINITION	UNIT
L	Length	m
t	Thickness	m
w	Width	m
m	Mass	kg
A	Area	m^2
V	Volume	m^3
ρ	Density	kgm^{-3}
r	Radius	m
F	Force	N
E	Young's modulus	Pa
G	Shear modulus	Pa
ν	Poisson ratio	$-$
τ_s	Shear stress	Pa
γ	Shear strain	$-$
θ	Angle of twist	rad
τ	Torque	Nm
f	Frequency	Hz
T	Time	s
ω	Angular velocity	s^{-1}
Δx	Transverse displacement	m
I	Mass moment of inertia	kgm^2
J	Torsion constant	m^4
κ	Torsion spring constant (kappa)	$Nm\,rad^{-1}$
z	Coupling parameter	$-$
R	Displaced distance	m
M_{tex}	Mass textile	kgm^{-2}

1 INTRODUCTION

This thesis focuses on obtaining the dynamic shear modulus of double clamped thin plates using a torsional pendulum. The approach of using the torsion test is to determine the shear modulus of a material because the torsional motion provides the pure form of shear stress in the material. Experimentally, the dynamic shear modulus is determined by means of a torsional pendulum. In addition, the testing method used in this thesis is non-destructive.

Material testing has gained importance over time. It is an essential step in the design and manufacturing processes. The primary purpose of the material testing is to make sure if the product will not go through any destructive failure in its service life.
Mechanical testing of materials is categorized into static and dynamic testing methods.

Static testing method is carried out by applying a known force or a moment to induce a deformation in a material [1]. It determines the ability of the material to withstand an applied load without failing at the ultimate breaking strength of the material.

Dynamic testing method is carried out by applying an oscillatory force and measuring the frequency of the wave. It tests sudden stress in the material by increasing the speed at which the force is imparted on the material. As a result, vibrational signal is obtained.

"Vibrational testing can help validate your design to see if it will survive its intended environment. It simulates a variety of transportation scenarios, operating environments, and the effect of external vibration within a storage environment." [2] Dynamic testing is widely used in aerospace industry. Aero planes encounter different environmental conditions such as temperature, pressure etc. It is preferred over static testing in aerospace industry as they go through real dynamic conditions. In aerospace industry, design plays an essential role along with the material properties. Dynamic testing is more valuable to understand the ability of the product from the design perspective.

"The mechanical strength of a material under a steadily increasing load can be determined in uniaxial tensile tests, compression (upsetting) tests, bend tests, shear tests, plane-strain tensile tests, plane strain compression (Ford) tests, torsion tests, and biaxial tests." [3]

1.1 Objectives

The aim of this thesis is to develop a simple and non-destructive engineering mechanism that measures the dynamic shear modulus of a desired material using torsional motion. The vibrational analysis is conducted by clamping both ends of the specimen and exerting torsional motion in the specimen.

This thesis will show the extraction for the value of a coupling parameter z, that is used to calculate the shear modulus using vibrational analysis and verify if it could be used for the specimen of different material and geometry. The value of the parameter z is due to the given boundary condition and shows the coupling of the two springs.

The mechanism will be designed and verified using Finite Element Analysis. The results will be compared to actual material property values. The virtual design will be manufactured and tested.

The thesis aims to find the solutions to following questions:

- How to find dynamic shear modulus of thin plates using torsional motion?
- Are FEA results trustworthy and how do they differ from the practically conducted test results?
- Does the mechanism behave same as the parallel connected springs that operate simultaneously?
- Is there a geometry dependent coupling parameter "z" that describes universally the torsional motion with two clamped ends?

1.2 Relevance of the topic

Material testing has gained importance with the development of the technology industry. This has improved the production in many ways e.g. production cost, quality, and reliability of the products. This thesis is a material study on functional properties. It develops new measurement technology for non-destructive and repeatable material characterization. Material aging must be tested because sustainability requires the lifetime estimation. So, repeatability allows for aging studies of materials and so forth contributes to

sustainable material engineering. It is essential to test and understand the material properties before utilizing them in manufacturing processes as this will predict the production outcome. Testing of materials can be categorized into two groups:

- Destructive Testing (DT)
- Non-Destructive Testing (NDT)

1.2.1 Destructive Testing

Destructive testing methods have been in use for a long time. They give an understanding of a specimen's behavior and effectiveness when the load is applied. DT methods involve damaging of the test specimen to get the material properties. There are different types of destructive testing such as fracture, fatigue, corrosion, mechanical testing, and residual stress measurement. They are easy to conduct and extract the information needed. It is used in testing large structures, automobile, and aircrafts. Destructive testing method is effective for mass produced items as it allows to have a statistical number of items to be destroyed to obtain the information.

1.2.2 Non-Destructive Testing

In non-destructive testing the test specimen does not go through any physical damage and maintains its state for later use. This is of great advantage when there are only a few items manufactured that are supposed to enter the market and need to be tested. Non-destructive testing will conserve the item even after it has gone through testing. NDT provides reliable results along with the benefit of being cost-efficient. It also allows to make amendments to improve the usage of products. Some of the NDT methods are Radiographic Testing, Ultrasonic Testing, Electromagnetic Testing, Visual Testing, Laser Testing Methods and Vibrational Analysis etc.

1.3 Reference to the existing standards

In this thesis, the calculation of dynamic shear modulus depends on the existing standard ASTM E1876-15 discussed later in section 2.1. IMCE, the company that carries out impulse excitation measurements is also using ASTM E1876-15 standard.

The equation for transverse vibration of homogenous isotropic prismatic bars is illustrated below [4],

$$E\, r_z^2\, \frac{\partial^4 v}{\partial x^4} + \rho\, \frac{\partial^2 v}{\partial t^2} - r_z^2\, \frac{\partial^4 v}{\partial x^2 \partial t^2} - r_z^2 \left(\frac{E}{K'G} \frac{\partial^4 v}{\partial x^2 \partial t^2} - \frac{\rho}{K'G} \frac{\partial^4 v}{\partial t^4} \right) = 0 \qquad (1)$$

$$\boldsymbol{Euler - Bernoulli} \qquad \boldsymbol{Rayleigh} \qquad \boldsymbol{Timoshenko}$$

Euler-Bernoulli is a linear beam theory that describes the bending motion but not torsional motion. Rayleigh theory and Timoshenko theory were added that describe the rotatory motion and shear deformation in the beam respectively.

In the case of this thesis, it is difficult to obtain different vibrating modes by solving any of the equations. The equation that has a solution does not contain rotation. Whereas, this thesis focuses on the obtaining shear modulus due to torsional motion.

According to IMCE, "Theoretically there is no analytical solution to Timoshenko's differential equation. In the early 1960's Spinner and Teft proposed following approximate equation:

$$E = 0.9465\, \rho\, f_r^2 \left(\frac{L^4}{t^2} \right) T_1 \qquad (2)$$

$E = Young's\ modulus\ (Pa)$

$\rho = density\ (kgm^{-3})$

$f_r^2 = flexural\ frequency\ (Hz)$

$L, t\ = length, thickness\ (m)$

$T_1 = correction\ factor$

This formula has been accepted as a standard: ASTM C 1259 – ASTM E 1876 – ISO 12680. Slightly modified in EN 843-2 (2006)" [4].

This shows that the standard is not based on any analytical derivation. Whereas, it is based on the experimental findings. Based on this reason, Finite Element Analysis method was used, as there is no other definite method to prove the results in this thesis. This standard does not consider viscous damping or material damping. This results in lower frequency and underestimated value for the dynamic shear modulus. The standard does not elaborate on the meaning of the correction factor T_1, other than the dimensions. The parameter T_1 could possibly be a compensation for the damping.

2 LITERATURE REVIEW

2.1 ASTM E1876-15

This standard test method is used to measure the Dynamic young's modulus, shear modulus and Poisson's ratio by Impulse Excitation Technique.

According to this standard, resonance frequency of a specimen with a specified geometry is measured by tapping the specimen and recording the induced signal with a microphone. The frequency is obtained from the time domain by conducting fast Fourier transformation. [5]

This method is not suitable for the lightweight materials. If the specimen is tapped with an impact force, the specimen will fly away. If it is tapped with less force, then there will be no induced signal. In case of bending, it can be made possible by clamping the specimen at one end. The cantilever beam will bend and vibrate freely. Therefore, lightweight materials can be tested but using different equations as different boundary conditions are applied.

To use this method for obtaining shear modulus, the specimen will have a fixed node point in the middle. This allows the twisting motion in the specimen.
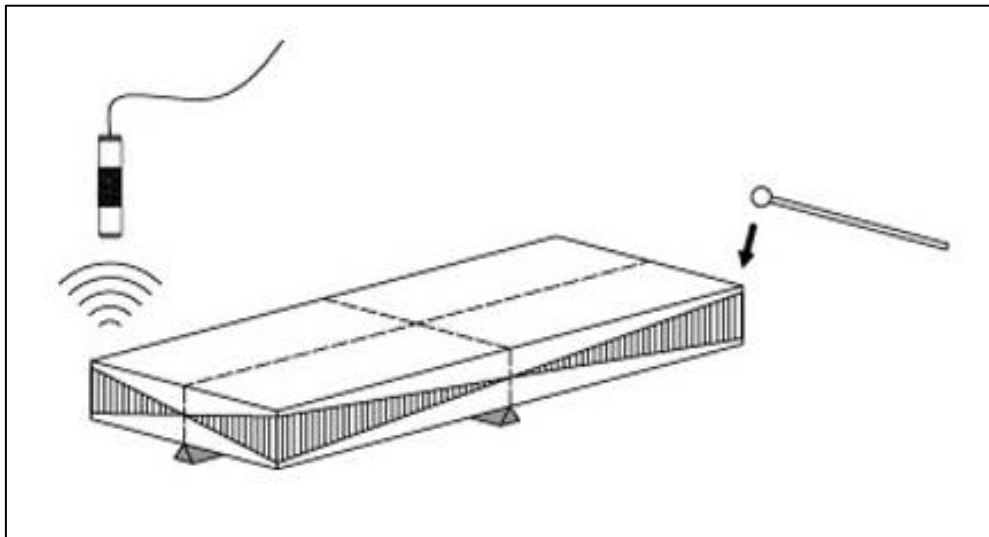
Figure 1: The equipment to measure the torsional vibration frequency [5]

The system measures the torsional vibration frequency. Shear modulus is obtained using the following equation [5],

$$G = \frac{4Lmf_t{}^2}{wt}R \qquad (3)$$

Where,

$G = shear\ modulus\ (Pa)$

$f_t = torsional\ frequency\ (Hz)$

$m = mass\ (kg)$

$L = length\ (m)$

$w = width\ (m)$

$t = thickness\ (m)$

$R = correction\ factor$

The equations used are for undamped motion. If there is damping in the system, this will give a measurement error. IMCE is presently working on removing all the viscous damping by using a vacuum chamber to minimize the measurement error.

This thesis uses the existing standard ASTM E1876-15. To minimize the error due to damping, external inertia is clamped at the node point of the specimen. This is an advantage for measuring the dynamic shear modulus as it will make the pendulum motion slower. The lower frequency effects the viscous damping by making it smaller or insignificant.

2.2 Shear Modulus

A numerical constant that defines the elastic properties of a material under the applied transverse internal forces is known as shear modulus. It describes the resistance of a material to shear deformation. Torque applied on an object results in the twisting about its lengthwise axis. This distorts even the smallest volume of that object in a way that parallel sliding of its two faces occur. It measures the resistant ability of the material to transverse deformations. [6]

Mathematically it can be defined as [7],

$$Shear\ modulus\ (G) = \frac{shear\ stress}{shear\ strain} \tag{4}$$

The SI unit for shear modulus is Pascals (Pa) and is often denoted as "G".

2.2.1 Shear stress

Shear stress is defined as the force acting tangent to a certain area. It is caused when the external loads cause the two sections of the body to slide over one another in the plane of an area. [7]

$$Shear\ stress = \frac{Shear\ force}{Area} = \tau_s = \frac{F}{A} \tag{5}$$

The SI unit for shear stress is Pascals (Pa).

2.2.2 Shear strain

When an external load is applied, the line segment not only go through the elongation and contraction, but the deformation causes them to change direction. The change in angle between two perpendicular line segments is known as shear strain. This angle is denoted by γ (gamma) and is measured in radians. [7]

It can also be represented as the tangent of the angle θ. [7]

$$Shear\ strain\ (\gamma) = \frac{transverse\ displacement}{initial\ length} = \frac{\Delta x}{l} = \tan\theta \tag{6}$$

2.3 Torsional spring

A spring that stores mechanical energy when it is twisted is known as torsional spring. In case of an elastic object mechanical energy is stored while twisting. The twisting motion caused by torque is known as torsion.

"Torque is a moment that tends to twist a member about its longitudinal axis." [7] This is illustrated in Figure 2. The grid showing the longitudinal and circular lines (figure a) distorts into the pattern when the torque is applied (figure b). The circles remain the same, whereas the longitudinal lines distort into a helix intersecting the circles at equal angles. [7]
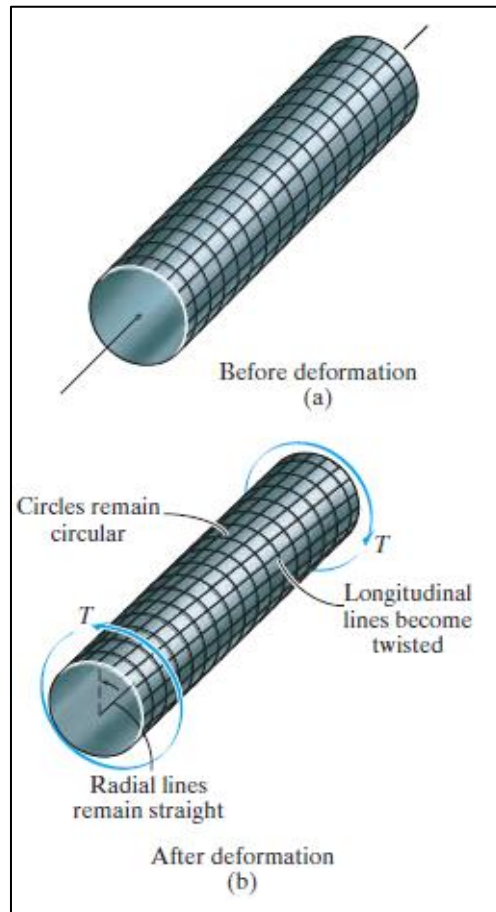
Figure 2: When torque is applied to a circular shaft [7]

If one end of the shaft is fixed and the torque is applied on the other end, the radial line on the cross section will rotate through an angle. This angle is known as the *angle of twist*. Mathematically it can be defined as, [7]

$$\theta = \frac{\tau L}{GJ} \qquad (7)$$

Where,

τ = Torque (Nm)

L = Length (m)

G = Shear modulus (Pa)

J = Torsion constant (m^4)
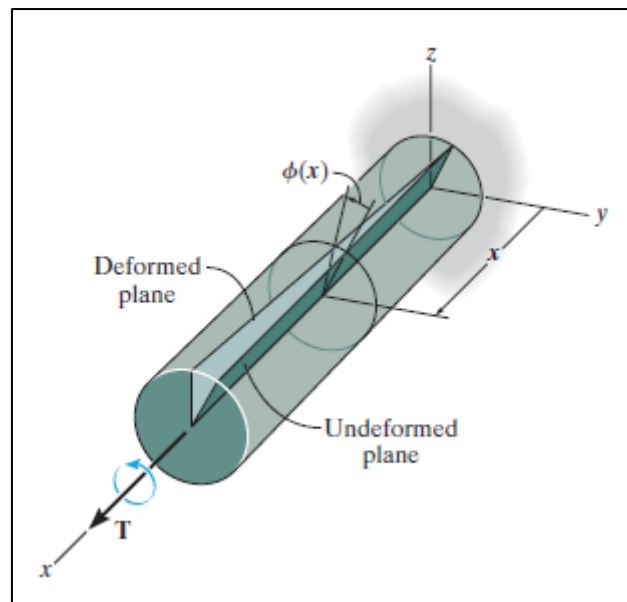
Figure 3: The increase in angle of twist as x increases [7]

2.3.1 Torsional spring constant

When a torsional spring is not twisted beyond its elastic limit, angular form of Hooke's law can be applied, [8]

$$\tau \propto \theta \qquad (8)$$
$$\tau = -\kappa\theta \qquad (9)$$

τ is the torque applied in Newton-meters, θ is the angle of twist in radians and κ (kappa) is the torsional spring constant in Newton-meters/radians.

18

2.3.2 Torsion constant

The term "torsion constant" is often confused with "Polar moment of inertia". Polar moment of inertia describes the resistance of a cylindrical shaft or beam to torsional deformation. Whereas, torsion constant is a term used for non-circular cross-sections or for the cross-sections where warping occurs to define their torsional stiffness. There is no exact analytical derivation for the torsion constant, whereas it is approximated. [9]

For example, the torsion constant for a rectangle is, [10]

$$J \approx \beta a b^3 \qquad (10)$$

Where,

a is the longer side

b is the shorter side

The SI unit for torsion constant is m^4.

Table 1: Approximation for the torsion constant of a rectangle [10]

a/b	β
1.0	0.141
1.5	0.196
2.0	0.229
2.5	0.249
3.0	0.263
4.0	0.281
5.0	0.291
6.0	0.299
10.0	0.312
∞	0.333

It is a property that is in relation with the applied torque and the angle of twist. In combination with the material properties and length, it defines the torsional stiffness. It can be illustrated as, [9]

$$\theta = \frac{\tau L}{G J_T} \qquad (7)$$
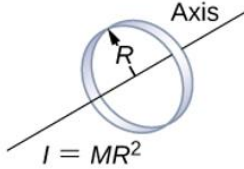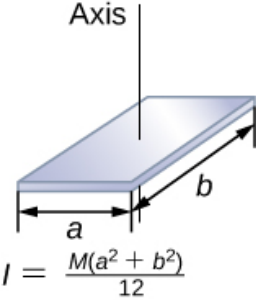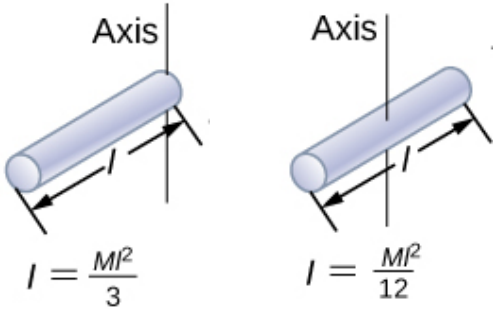
2.4 Mass moment of Inertia

Mass moment of inertia also known as rotational inertia, measures the resistance against angular acceleration. In case of a simple pendulum, the moment of inertia is defined in terms of mass of the pendulum and its distance r from the central point. [11]

The unit for mass moment of inertia is kgm^2.

Table 2 illustrates the mass moment inertia of different geometries used in this thesis work.

Table 2: Illustration of mass moment of inertia of different geometries [12]

Mass moment inertia of a point mass	$I = MR^2$
Mass moment inertia of a rectangle	$I = \dfrac{M(a^2 + b^2)}{12}$
Mass moment inertia of a rod	$I = \dfrac{Ml^2}{3}$ $\quad$ $I = \dfrac{Ml^2}{12}$

Mass moment of inertia relies on how the mass is distributed from its axis of rotation. It will increase if the mass is far from its axis of rotation. It becomes more challenging to change the velocity of rotational system if the mass is further away than the axis of rotation. This is proven in the later section 4.3 where parallel axis theorem is used by displacing the mass and calculating the mass moment of inertia.

2.5 Parallel Axis Theorem

The parallel axis theorem "states that the moment of inertia of an area about an axis is equal to the area's moment of inertia about a parallel axis passing through the "centroid" plus the product of the area and the square of the perpendicular distance between the axes." [7]
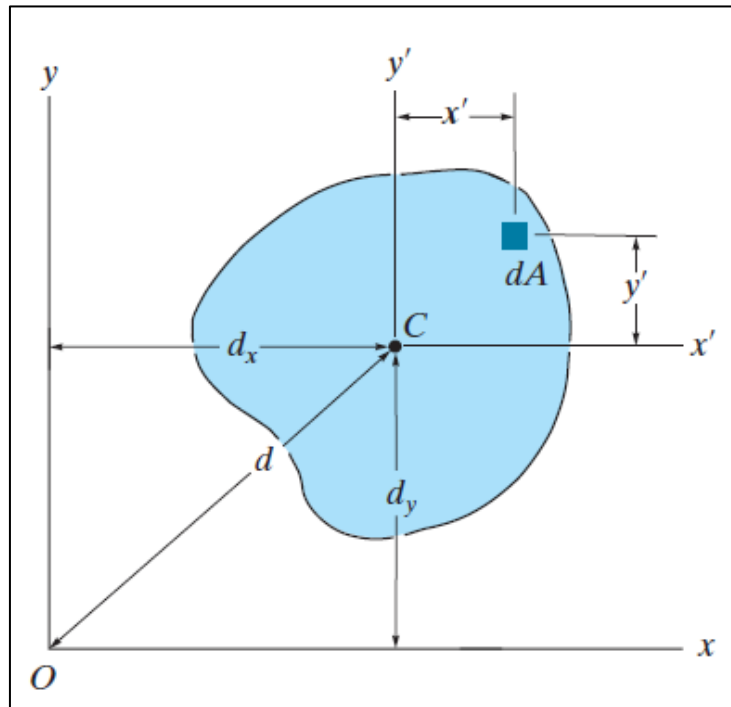
Figure 4: Illustration of parallel axis theorem corresponding to the equation [7]

Figure above illustrates the phenomenon of parallel axis theorem. To find the moment of inertia of the differential element dA, the perpendicular distance between the two axes d_y must be considered, as dA is not located in the mid-plane. Thus, the moment of inertia of the differential element will be, [7]

$$I_x = \bar{I}_{x\prime} + Ad_y{}^2 \qquad\qquad (11)$$

Whereas, $\bar{I}_{x\prime}$ is the moment of inertia of an element in the neutral axis.

If a rotating system comprises of many parts, then the total mass moment inertia is calculated using the parallel axis theorem because every part is displaced by a certain distance from the axis of rotation. So, the sum of all the inertias found using the parallel axis theorem will be the total mass moment of inertia of the rotating system.

3 METHOD

3.1 Undamped Torsional Pendulum

When a spring with one fixed end and the other end suspended is disturbed, it will go through an oscillatory motion under the restoring force of the spring. If the spring follows the Hooke's law i.e. force is proportional to the spring's extension, then the system is called simple harmonic oscillator (SHO). If the restoring force is in torsion, then this simple harmonic oscillator is known as a torsional pendulum. [13]

$$\tau = -\kappa\theta \qquad (9)$$

Where,

$\tau =$ Torque (Nm)

$\theta =$ Angle of twist (radians)

$\kappa =$ Torsional spring constant, kappa ($Nmrad^{-1}$)

Simple harmonic motion is periodic. The period of oscillation is given by, [14]

$$T = 2\pi\sqrt{\frac{I}{\kappa}} \qquad (12)$$

Where,

$T =$ Time for one oscillation (s)

$I =$ Mass moment of inertia (kgm^2)

$\kappa =$ Torsional spring constant, kappa ($Nmrad^{-1}$)

The angular frequency at which the spring oscillates is, [14]

$$\omega = 2\pi f = \frac{2\pi}{T} \qquad (13)$$

The equation (12) for undamped angular frequency can be written as,

$$\omega_0 = \sqrt{\frac{\kappa}{I_{external}}} \qquad (14)$$

The angle of twist is determined using the following equation,

$$\theta = \frac{\tau L}{GJ} \qquad (7)$$

By substituting θ in equation (9),

$$\kappa = \frac{GJ}{L} \qquad (15)$$

Substituting κ in equation (14),

$$\omega_0 = \frac{2\pi}{T} = \sqrt{\frac{\kappa}{I_{external}}} = \sqrt{\frac{GJ}{LI_{external}}} \qquad (16)$$

Where,

G = Shear modulus (Pa)

J = Torsion constant (m^4)

L = Length of the spring (m)

$I_{external}$ = Mass moment of inertia (kgm^2)

This equation is correct for one sided clamped specimen. For both sides clamped specimen, a constant z is included in the equation.

$$\omega_0 = 2\pi f = \sqrt{\frac{GJ\ z}{LI_{external}}} \qquad (17)$$

The mechanism involves two springs compared to one spring. This constant value is calculated in chapter **4.3**.

Educational torsional pendulum found in Arcada was used to find the torsional spring constant (kappa) by mounting a mass with a known polar mass moment of inertia, on the torsion axle and oscillated for a time period.
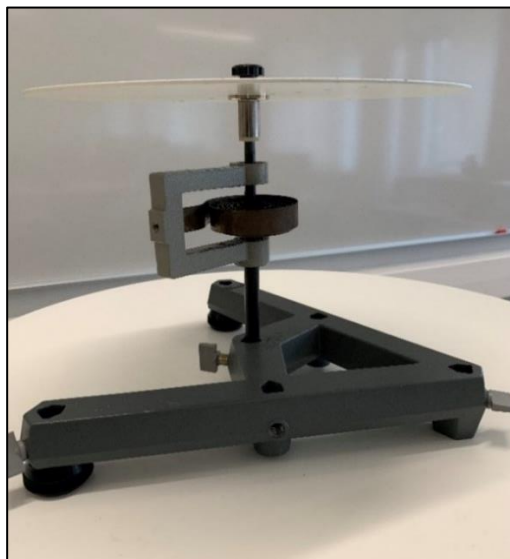
Figure 5: Educational torsional pendulum

The time period and the known inertia will determine the torsional spring constant. This torsional spring constant can be used to find any unknown inertias. The experiment is discussed in chapter **4.1**.

3.1.1 Torsional spring has no Mass Moment of Inertia
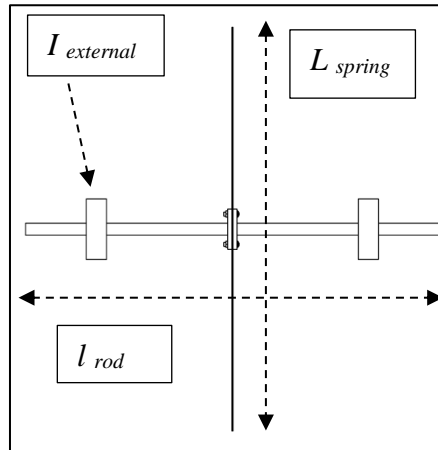
Figure 6: Schematic of the torsional pendulum

If the mass of the rectangular torsional spring is much smaller than the mass of the external mass moment of inertia, then the equation is written as,

$$\omega_0 = \frac{2\pi}{T} = \sqrt{\frac{GJz}{LI_{ext}}} \qquad (17)$$

Torsion constant for a rectangle $= J = \beta w t^3$

β value is used according to the ratio of width to thickness. If the ratio is higher than 10, the β value is $\frac{1}{3}$.

$$\omega_0 = \frac{2\pi}{T} = \sqrt{\frac{G\beta w t^3\, z}{LI_{ext}}} \qquad (18)$$

3.1.2 Torsional spring has Mass Moment of Inertia

If the mass of the rectangular torsional spring is not smaller than the mass of the external mass moment of inertia, then the inertia of spring is considered.

$$\omega = \frac{2\pi}{T} = \sqrt{\frac{G\beta w t^3\, z}{L(I_{external} + I_{spring})}} \qquad (19)$$

3.2 Finite Element Analysis (FEA)

"The Finite Element Analysis (FEA) is the simulation of any given physical phenomenon using the numerical technique called Finite Element Method (FEM)." [15]

FEA has expanded overtime as the technology industry has started to have a huge impact on the economy. FEA provides the numerical solution for the prediction of the product's behavior under given conditions. [15] It reduces the production time, material and cost by analyzing the design and optimizing it.

3.2.1 Eigen modes by COMSOL Multiphysics

COMSOL Multiphysics is a simulation software product that solves the engineering and scientific problems as closely as possible to the physical applications. It is an environment for simulation of scientific models for acoustics, electromagnetics, chemical reactions, mechanics, fluid flow and heat transfer.

One of the studies that can be simulated in COMSOL Multiphysics is Eigenfrequency analysis. Eigenfrequency analysis is conducted to determine frequencies for a consecutive analysis for a dynamic response. "Eigenfrequencies or natural frequencies are certain discrete frequencies at which a system is prone to vibrate." [16]

The deformation in the structure appear due to its vibration at a certain eigenfrequency. It deforms into a corresponding shape, known as the eigenmode. This analysis does not provide the size of the deformation. The deformation size can be found if the damping properties for an actual excitation are known. [16]

Figure 7 shows the eigen modes that corresponds to the numeric solutions of the following equation,

$$E\, r_z^2\, \frac{\partial^4 v}{\partial x^4} + \rho\, \frac{\partial^2 v}{\partial t^2} - r_z^2\, \frac{\partial^4 v}{\partial x^2 \partial t^2} - r_z^2 \left(\frac{E}{K'G} \frac{\partial^4 v}{\partial x^2 \partial t^2} - \frac{\rho}{K'G} \frac{\partial^4 v}{\partial t^4} \right) = 0 \qquad (1)$$
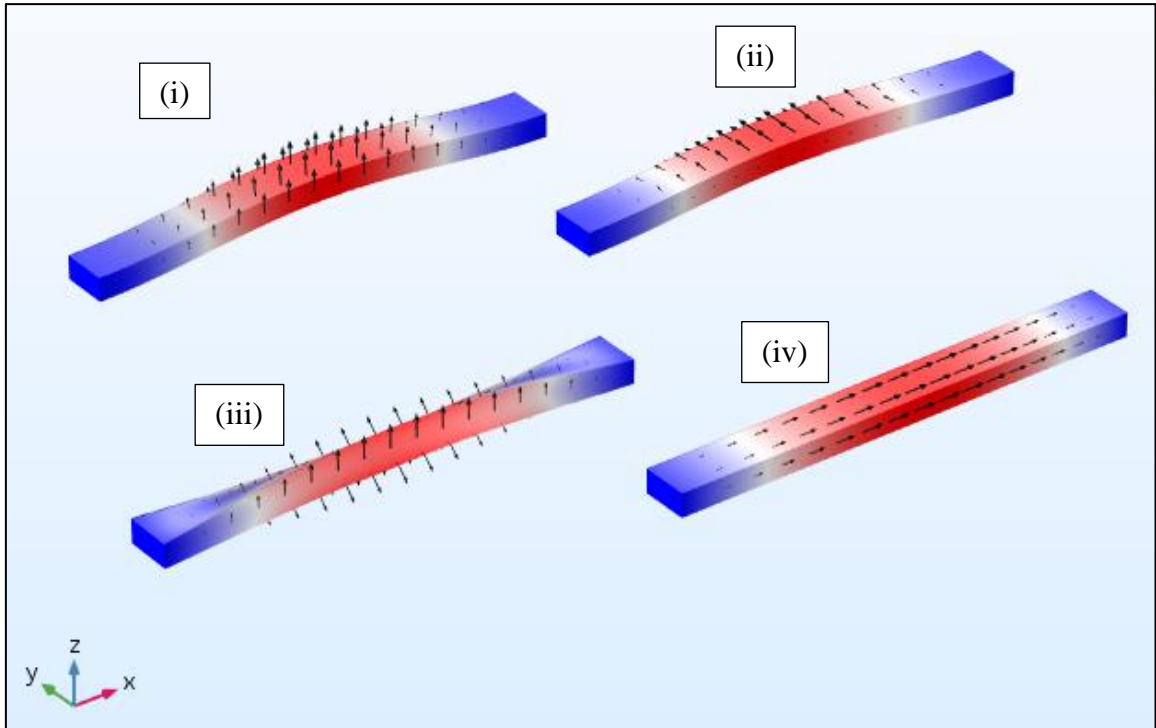
Figure 7: Different eigen modes for double clamped specimen [17]

The figure above shows different Eigenmodes for a doubly clamped beam.

(i)   Eigen mode for bending in z-direction (E_{bend})

(ii)   Eigen mode for bending in y-direction (E_{bend})

(iii)   Eigen mode for twisting (G)

(iv)   Eigenmode as the object contracts periodically (E_{young})
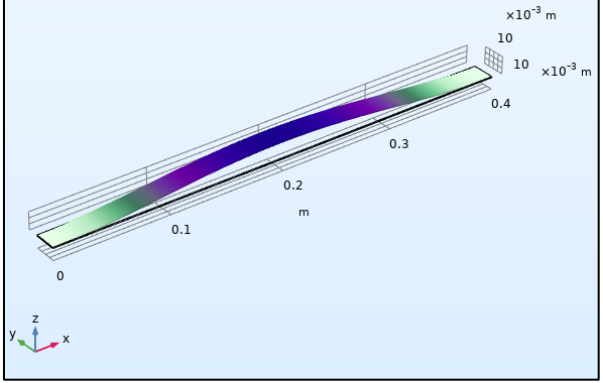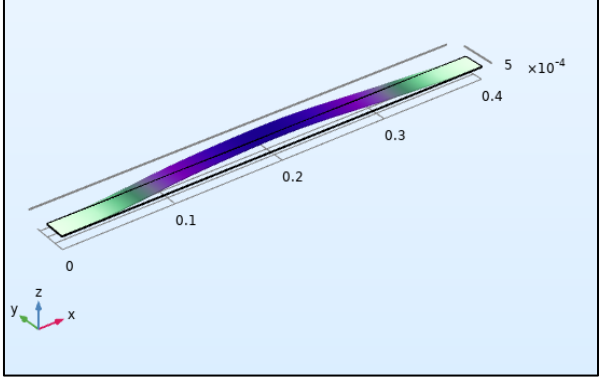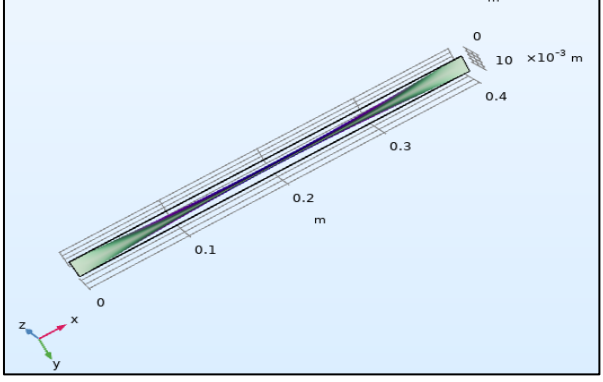
A rectangular beam was designed in SolidWorks and imported to COMSOL Multiphysics. The material given to the beam was Steel AISI 4340. Under structural mechanics, fixed constraints were added at both ends.

Table 3: Dimensions and density of the test specimen

Parameter	Value
Length (m)	0.4
Width (m)	0.02
Thickness (m)	0.001
Density of the material (kgm^{-3})	7850

26

Eigenfrequency study was conducted. The study provides eigenfrequencies for different modes i.e. bending in two different axis and twisting motion.

Table 4:Eigen modes of double clamped specimen in COMSOL Multiphysics

Eigen mode	Eigenfrequency (Hz)	Figure
First mode of bending in z-direction	33.238	
First mode of bending in y-direction	647.01	
First mode of twisting	409.55	

4   RESULTS

The purpose of this experiment is to establish the torsional spring constant κ by measuring the time T of an oscillation for a given mass moment of inertia I.

$$T = 2\pi \sqrt{\frac{I}{\kappa}} \qquad (12)$$

4.1   Educational pendulum and Parallel Axis Theorem
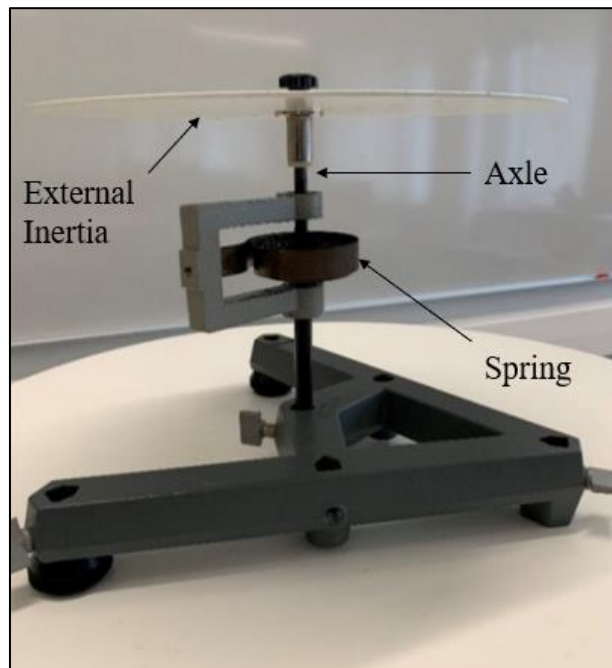
Figure 8: Educational torsional pendulum

- The experiment was conducted using different mass and geometry.
- The mass was placed on the torsion axle.
- Then, it was rotated by 180 degrees and released.
- As soon as it was released, the time measurement was started using a stopwatch.
- The number of oscillations were counted for some oscillations.
- After getting the time and number of oscillations, the period T of oscillation is calculated.
- The experiment was conducted several times using the same specimen to minimize the error.
- The process was repeated by placing a sphere, a disk, a solid cylinder and a hollow cylinder.

4.1.1 Wooden disk

Figure 9: Educational torsional pendulum with wooden disk

After carrying out the time measurement, the period of oscillation was calculated.

$$Period\ of\ oscillation\ (T) = \frac{Total\ time}{Number\ of\ oscillations}$$

Mass moment of inertia of the wooden disk is calculated using the equation, [12]

$$I = \frac{1}{2}mr^2 \qquad (20)$$

$mass = m = 0.2715\ kg$

$radius = r = 0.1125\ m$

After calculating average time and mass moment of inertia, torsional spring constant is determined using the equation,

$$T = 2\pi\sqrt{\frac{I}{\kappa}} \qquad (12)$$

Table 5: Measurement data for wooden disk

No. of oscillations	Total T (s)	T (1 oscillation) (s)	Average T (s)	I (kgm^2)	κ (Nm)
4	6.1	1.525	1.501733	0.001718	0.000309
5	7.48	1.496			
5	7.53	1.506			
6	8.93	1.488			
6	8.96	1.493			

4.1.2 Solid sphere

Figure 10: Educational torsional pendulum with solid sphere

Mass moment of inertia of a solid sphere is calculated using the equation, [12]

$$I = \frac{2}{5} m r^2 \qquad (21)$$

$mass = m = 0.968 \ kg$

$radius = r = 0.075 \ m$

Table 6: Measurement data for solid sphere

No. of oscillations	Total T (s)	T (1 oscillation) (s)	Average T (s)	I (kgm^2)	κ (Nm)
4	6.6	1.65	1.609333	0.002178	0.000341
5	8.1	1.62			
5	7.53	1.506			
5	8.27	1.654			
6	9.7	1.616			

4.1.3 Solid cylinder

Figure 11: Educational torsional pendulum with solid cylinder

Mass moment of inertia of a solid cylinder is calculated using the equation, [12]

$$I = \frac{1}{2}mr^2 \qquad\qquad (20)$$

$mass = m = 0.4225 \ kg$

$radius = r = 0.045 \ m$

Table 7: Measurement data for solid cylinder

No. of oscillations	Total T (s)	T (1 oscillation) (s)	Average T (s)	I (kgm^2)	κ (Nm)
4	3.32	0.83	0.836403	0.000428	0.000248
4	3.35	0.837			
5	4.3	0.86			
5	4.19	0.838			
6	5.08	0.846			
8	6.45	0.806			

4.1.4 Hollow cylinder

Figure 12: Educational torsional pendulum with hollow cylinder

Mass moment of inertia of a hollow cylinder is calculated using the equation, [12]

$$I = mr^2 \qquad (22)$$

$mass = m = 0.4391 \, kg$

$radius = r = 0.045 \, m$

Table 8: Measurement data for hollow cylinder

No. of oscillations	Total T	T (1 oscillation)	Average T	I	κ
	(s)	(s)	(s)	(kgm^2)	(Nm)
4	4.24	1.06	1.065433	0.000889	0.000317
4	4.33	1.082			
5	5.35	1.07			
5	5.29	1.058			
6	6.34	1.056			

The table below shows the value of torsional spring constant κ obtained using different mass moment of inertia. The value of κ obtained using solid cylinder with the lower mass moment of inertia is not like the other κ values. Whereas, the κ value obtained using the item with higher mass moment of inertia have higher precision.

Table 9: Mass moment of inertia and Torsional spring constant for different shapes

Item	Mass Moment of Inertia (kgm^2)	κ (Nm)
wooden disk	0.001718	0.000309
solid sphere	0.002178	0.000341
solid cylinder	0.000428	0.000248
hollow cylinder	0.000889	0.000317

The inaccuracy appeared due to the systematic error of the clock operator as it is possible to count wrong while the motion is fast in the case of the objects with lower mass moment of inertia. For example, the solid cylinder was oscillating fast at an average of 0.83 seconds per oscillation.

Secondly, the setup for the cylinders is different than the disk and the sphere. It includes a holding disk and a screw. Its inertia has not been considered. This could also be a possible reasoning behind the difference in the κ value.

The slight inaccuracy in κ value could also be due to the significance of viscous damping. The items with higher mass moment of inertia were oscillating slower. As the pendulum motion is slower, there will not be any meaningful air resistance. The lower frequencies reduced the systematic error by neglecting the viscous damping. External inertia should have higher density, longer cross section and longer length to obtain lower frequencies and to make the damping constant (zeta ζ) insignificant.

4.1.5 Verification of the parallel axis theorem

Figure 13: Educational torsional pendulum with metal disk

Mass moment of inertia of a thin metal disk is calculated using the equation,

$$I_o = \frac{1}{2}mr^2 \qquad (20)$$

$mass = m = 0.403\ kg$

$radius = r = 0.15\ m$

Educational torsional pendulum was used to prove the parallel axis theorem.

$$I = I_o + mR^2 \qquad (23)$$

The disk was rotated at 180° from the equilibrium position and released. The time was measured for several oscillations. This was done multiple times by mounting the disk on the torsional axle at a distance R i.e. 0.003, 0.006, 0.009 and 0.012 m from the center of the rotating disk and the central axis as shown in Figure 14. The table shows the results obtained from the experiment.
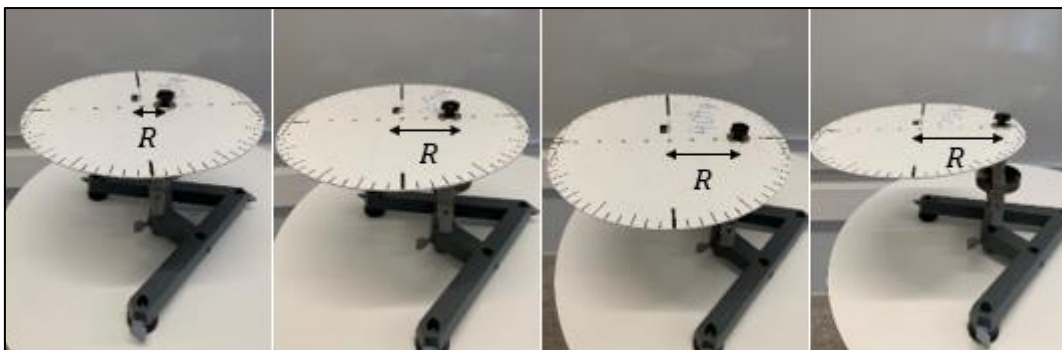
Figure 14: Parallel axis theorem using the metal disk on torsional pendulum

Table 10: Measurement data for parallel axis theorem

Distance (m)	No. of oscillations	Total T (s)	T (1 oscillation) (s)	Average T (s)
0	4	9.84	2.46	2.4313
	4	9.83	2.4575	
	5	12.12	2.424	
	5	12.2	2.44	
	6	14.25	2.375	
0.003	5	12.72	2.544	2.545543
	5	12.69	2.538	
	6	15.3	2.55	
	7	17.8	2.542857	
	7	17.87	2.552857	
0.006	5	14.2	2.84	2.808
	6	16.8	2.8	
	6	16.9	2.816667	
	7	19.6	2.8	
	6	16.7	2.783333	
0.009	5	16.38	3.276	3.202333
	6	19.06	3.176667	
	6	19.39	3.231667	
	6	18.75	3.125	
0.012	5	18.54	3.708	3.670167
	4	14.93	3.7325	
	5	17.85	3.57	

The parallel axis theorem is proven if there is a linear relationship between the time T and the distance R.

$$I = I_o + mR^2 \qquad (23)$$

$$T = 2\pi \sqrt{\frac{I}{\kappa}} \qquad (12)$$

$$\left(\frac{T}{2\pi}\right)^2 = \frac{I}{\kappa}$$

$$\left(\frac{T}{2\pi}\right)^2 \kappa = I \qquad (24)$$

Substituting I in equation (23) gives,

$$\left(\frac{T}{2\pi}\right)^2 \kappa = I_o + mR^2$$

$$T^2 = \frac{(2\pi)^2}{\kappa}\left(\frac{1}{2}mr^2 + mR^2\right)$$

$$T^2 = \frac{(2\pi)^2}{\kappa} m\left(\frac{1}{2}r^2 + R^2\right) \qquad (25)$$

This is the linearized equation with the substitution of T^2 as y and R^2 as x.

$$y = c + kx \qquad (26)$$

$$y = T^2, \qquad c = \frac{1}{2}r^2 m \frac{(2\pi)^2}{\kappa}, \qquad k = \frac{(2\pi)^2}{\kappa} m, \qquad x = R^2$$

The plot of x and y should be linear to prove the parallel axis theorem.

Table 11:Time squared vs distance R squared

R	T^2	R^2
(m)	(s^2)	(m^2)
0	5.91122	0
0.003	6.479788	0.000009
0.006	7.884864	0.000036
0.009	10.25494	0.000081
0.012	13.47012	0.000144
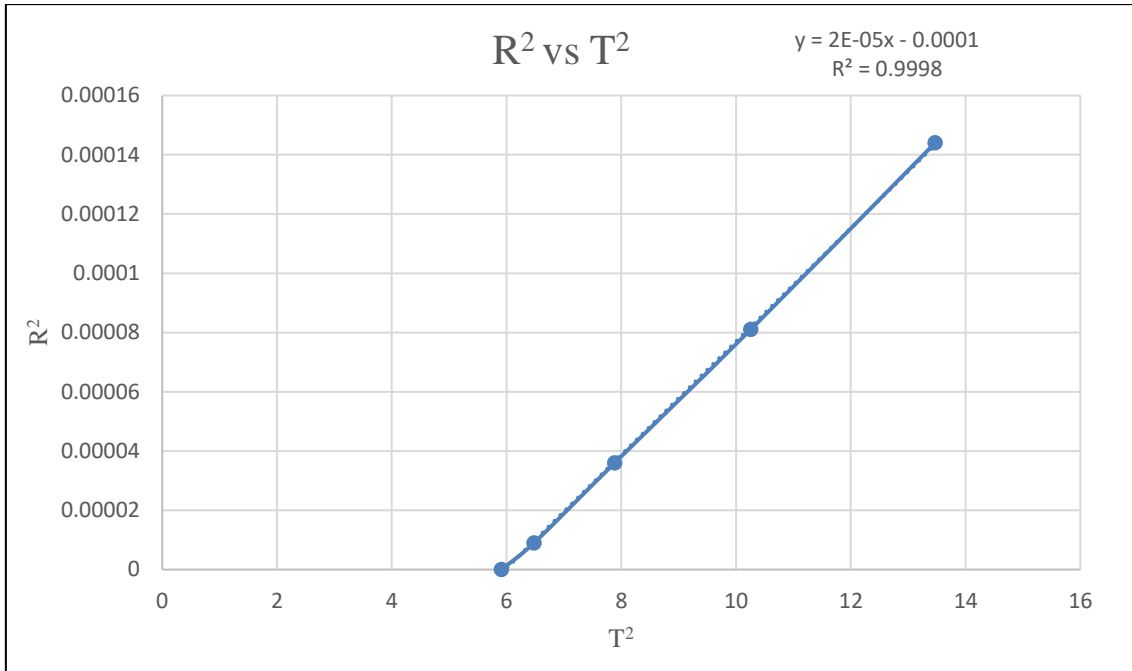
Figure 15: Distance R squared vs Time squared

The graph above proves the parallel axis theorem. By increasing the distance from the center of the rotating disk to the central axis makes the oscillation time slower. To make the viscous damping insignificant, the frequencies obtained should be low.

4.2 COMSOL study of a plate fixed at both ends

Before manufacturing the device, it had to be verified using Finite Element Analysis. COMSOL Multiphysics was used to verify the design.

A rectangular specimen of 1 mm thickness with a width of 20 mm and length of 400 mm was designed in SolidWorks. A rod fixture with a diameter of 12 mm and 200 mm long is attached on both sides of the specimen. A fillet feature was added on the fixture. The SolidWorks part file was saved as stl format and imported to COMSOL Multiphysics.
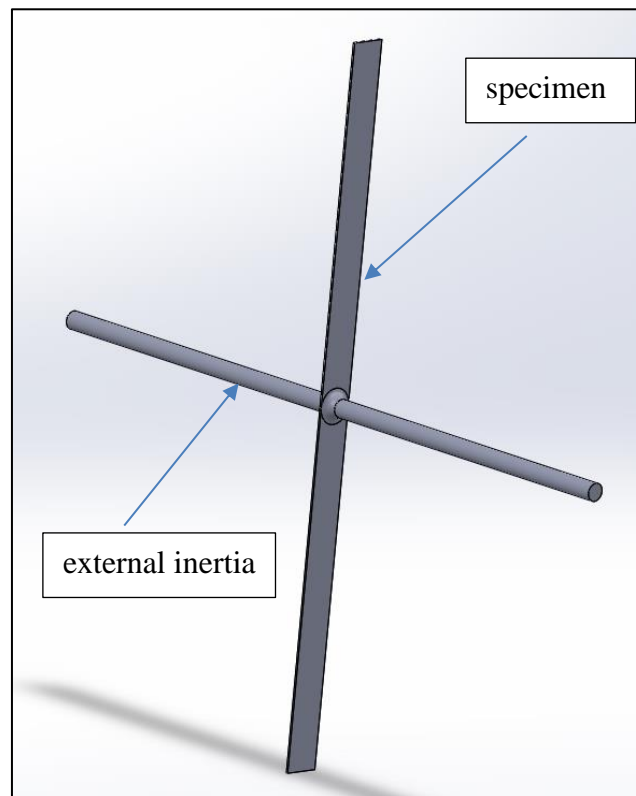
Figure 16: Initial design for testing the COMSOL Multiphysics

The part was given the material of Steel AISI 4340. COMSOL Multiphysics provides the properties for all the materials.

Figure 17: Properties of Steel AISI 4340 from COMSOL

Using the Young's modulus (E) and Poisson's ratio (v), shear modulus (G) can be calculated. [18]

$$G = \frac{E}{2(1 + v)} \qquad (27)$$

$$= \frac{205\ GPa}{2(1 + 0.28)} = \boldsymbol{80.07\ GPa}$$

Both ends of the spring were clamped using the fixed constraints under Solid Mechanics. They are indicated by the arrows in Figure 18. This will make the twisting mode significant and suppress the other modes of vibration.

After adding the tetrahedral mesh (normal size) to the part, Eigenfrequency study was conducted. The study gives different modes like bending, extension, torsion etc. The Eigenfrequency for the spring in torsion was reported.
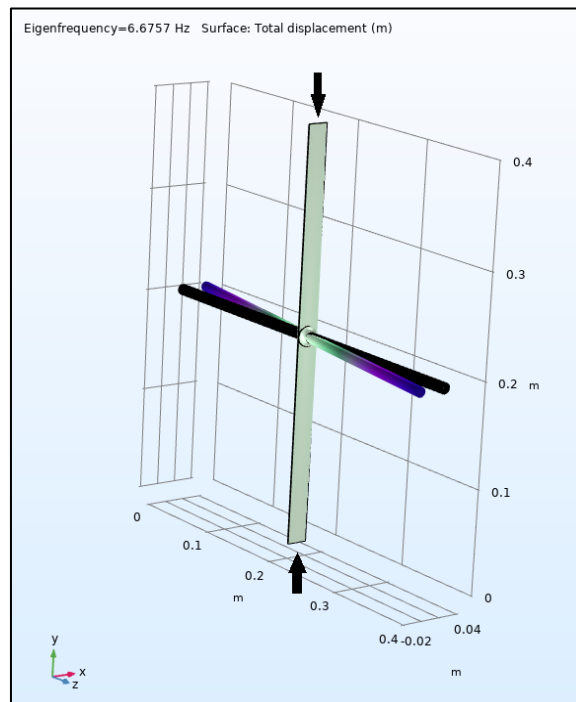
Figure 18: Eigenfrequency study conducted in COMSOL Multiphysics

39

4.2.1 COMSOL study with varying length of the rod
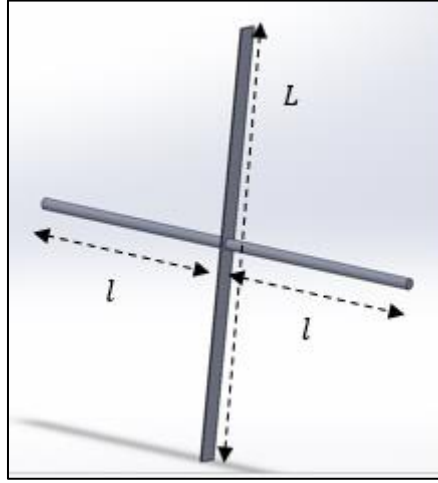
Figure 19: FEA conducted by varying the length (l) of the rod

$$\omega = \frac{2\pi}{T} = \sqrt{\frac{\kappa}{I_{external}}} \qquad (14)$$

$$\kappa = \frac{GJ}{L} \qquad (15)$$

Torsion constant for a rectangle $= J = \beta w t^3 \qquad \beta = \frac{1}{3} \qquad (10)$

Mass moment of inertia of an external mass [14] $= I_{ext} = \frac{1}{12} m l^2 \qquad (28)$

$$\omega = 2\pi f = \sqrt{\frac{G\beta w t^3 \, z}{L \frac{1}{12} m l^2}} = \sqrt{\frac{G \frac{1}{3} w t^3 \, z}{L \frac{1}{12} m l^2}} = \sqrt{\frac{4 G w t^3 \, z}{L m l^2}} \qquad (29)$$

The mass is calculated using density of the material and the volume, [19]

$$\rho = \frac{m}{V} = \frac{m}{Al} \qquad , m = \rho Al \qquad (30)$$

Substituting mass m in equation,

$$\omega = 2\pi f = \sqrt{\frac{4 G w t^3 \, z}{L \rho Al \times l^2}} = \sqrt{\frac{4 G w t^3 \, z}{L \rho Al^3}} \qquad (31)$$

Theoretically, this equation shows that the frequency f is directly proportional to the $\sqrt{\frac{1}{l^3}}$.

$$f \propto \sqrt{\frac{1}{l^3}} \qquad (32)$$

40

The FEA study is conducted to prove this theory. The COMSOL study was conducted in the same manner by increasing the length of the rod from 0.2 m to 0.6 m. The material given to the mechanism was Steel AISI 4340 and the test specimen was clamped at both ends. The eigen frequencies obtained from the COMSOL are as follows:

Table 12: Eigenfrequency obtained for different length of the rod

Length l of the rod (m)	Frequency f (Hz)
0.2	6.6757
0.3	3.6625
0.35	2.9135
0.4	2.3783
0.45	1.9929
0.5	1.6725
0.55	1.4725
0.6	1.2959

The values for $\sqrt{\dfrac{1}{l^3}}$ were plotted against the frequencies. The graph below shows the linear relationship between the frequency f and $\sqrt{\dfrac{1}{l^3}}$.
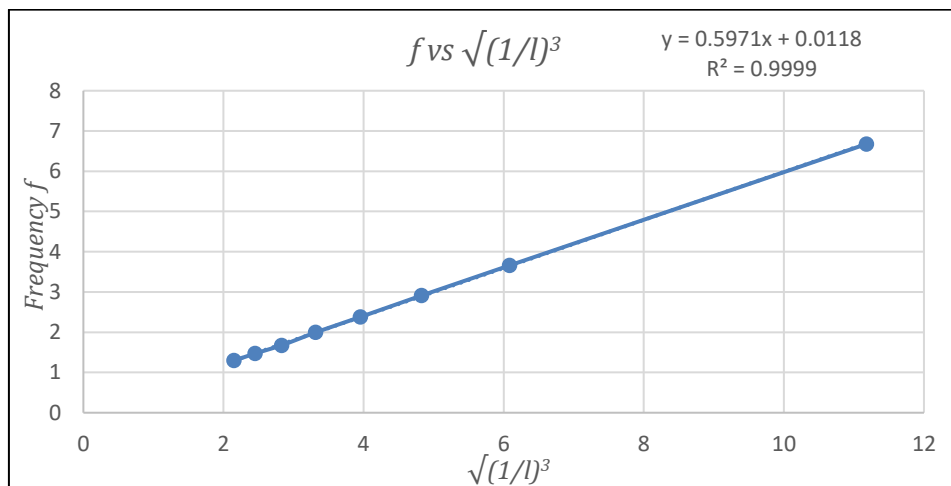
Figure 20: Dependence of frequency on the length of the rod

This linear relationship shows that $f \propto \sqrt{\dfrac{1}{l^3}}$ i.e. if the length increases, frequency decreases.

41

4.2.2 COMSOL study without the fillet
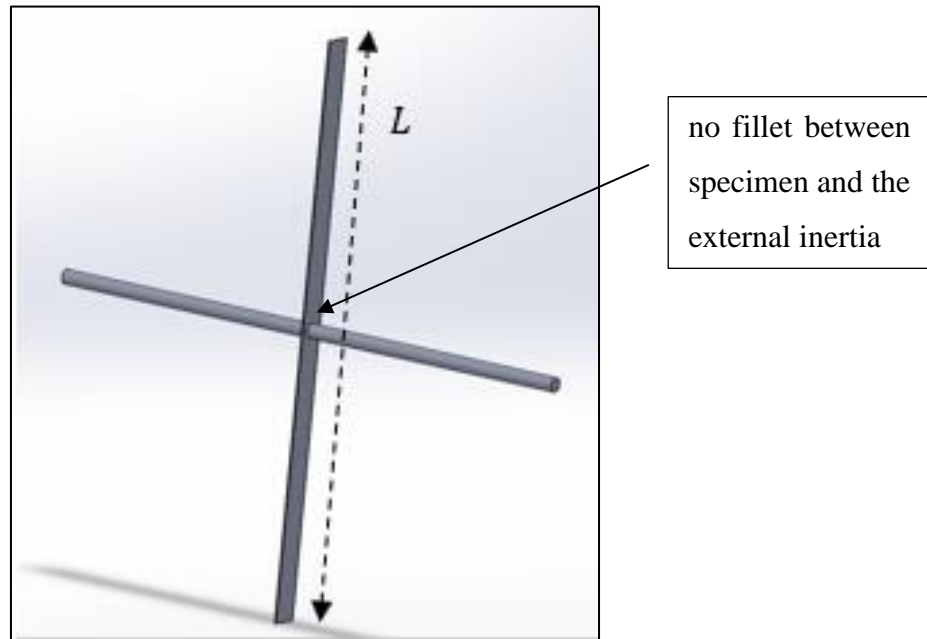
Figure 21: Design with no fillet added between the specimen and the rod

A study was conducted using the design with no fillet added. This was done to verify that the COMSOL results are trustworthy.

Table 13: Eigenfrequencies obtained with different feature in the design

Length l of the rod (m)	Frequency f (no fillet) (Hz)	Frequency f (fillet) (Hz)
0.3	3.591	3.6625
0.4	2.3356	2.3783
0.5	1.6673	1.6725
0.6	1.2748	1.2959

COMSOL study for the design without the fillet gave eigen frequency slightly higher than the study for the design with the fillet. A slight difference in the results show that the results obtained from COMSOL are not just numbers generated by the software but are reliable.

4.2.3 COMSOL study with different materials

Using COMSOL Multiphysics, the analysis was conducted using different materials. The material given to the spring was Aluminum with a density of 2700 kgm^{-3} and the material given to the rod was Steel AISI 4340 with a density of 7850 kgm^{-3}. The fixed constraints were added on the both sides of the spring so that it is clamped from both ends. The eigen frequency study was conducted, following the eigen mode for torsion. Eigen frequencies obtained using lighter material for the spring compared to the rod gave lower eigen frequencies.

Table 14: Frequencies obtained using different materials for different lengths

Length of the rod (m)	Frequency -different materials (Hz)	Frequency - same material (Hz)
0.3	2.1078	3.6625
0.4	1.3851	2.3783
0.5	0.97913	1.6725
0.6	0.75282	1.2959

The values for $\sqrt{\dfrac{1}{l^3}}$ were plotted against the frequencies.

Table 15: Frequency with respect to the change in length of the rod

Length of the rod (m)	Frequency -different materials (Hz)	$\sqrt{\dfrac{1}{l^3}}$ $(m^{-\frac{3}{2}})$
0.3	2.1078	6.085806
0.4	1.3851	3.952847
0.5	0.97913	2.828427
0.6	0.75282	2.151657

The graph below shows the linear relationship between the frequency f and $\sqrt{\dfrac{1}{l^3}}$.
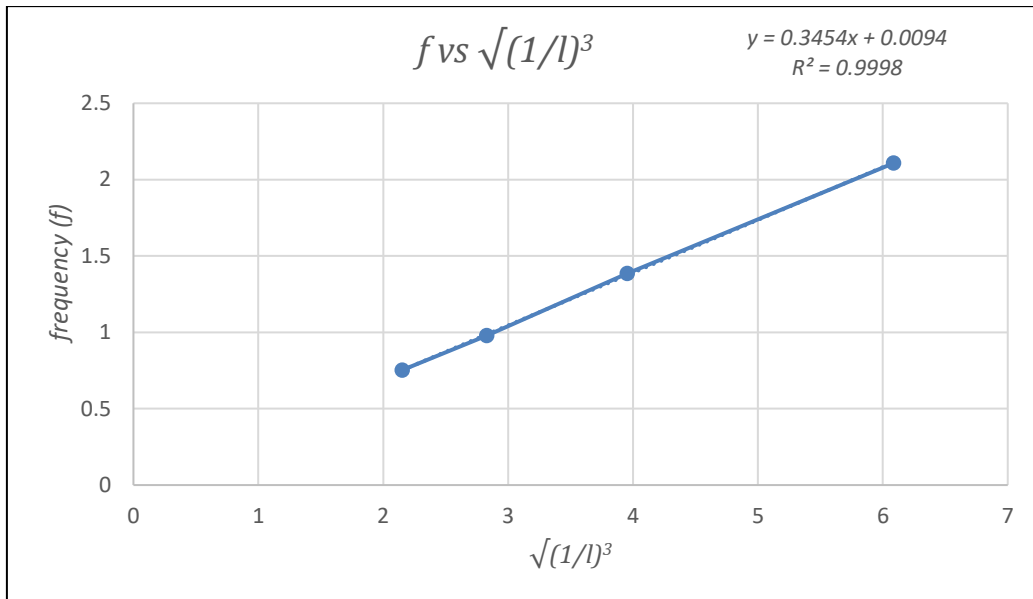
Figure 22: Dependence of frequency on the varying length for different materials

This graph verifies the study conducted in COMSOL by giving different materials to the inertia and the spring. By adding different materials to the spring and the inertia, the linear relationship between frequency and length is proven.

4.3 COMSOL study with engineered external inertia

For accurate results, viscous damping must be made irrelevant to this study. This is achieved by making the pendulum motion slower i.e. the frequencies obtained should be low. As it moves slower, there will not be any meaningful air resistance. This is done by increasing the external inertia.

The design was modified by adding two mass rings to both the rods. The rods were fixed to the connector plates. COMSOL analysis was conducted by moving the mass rings using the parallel axis theorem from the difference of 5 mm from the connector plate to the other end of the rod at 180 mm.
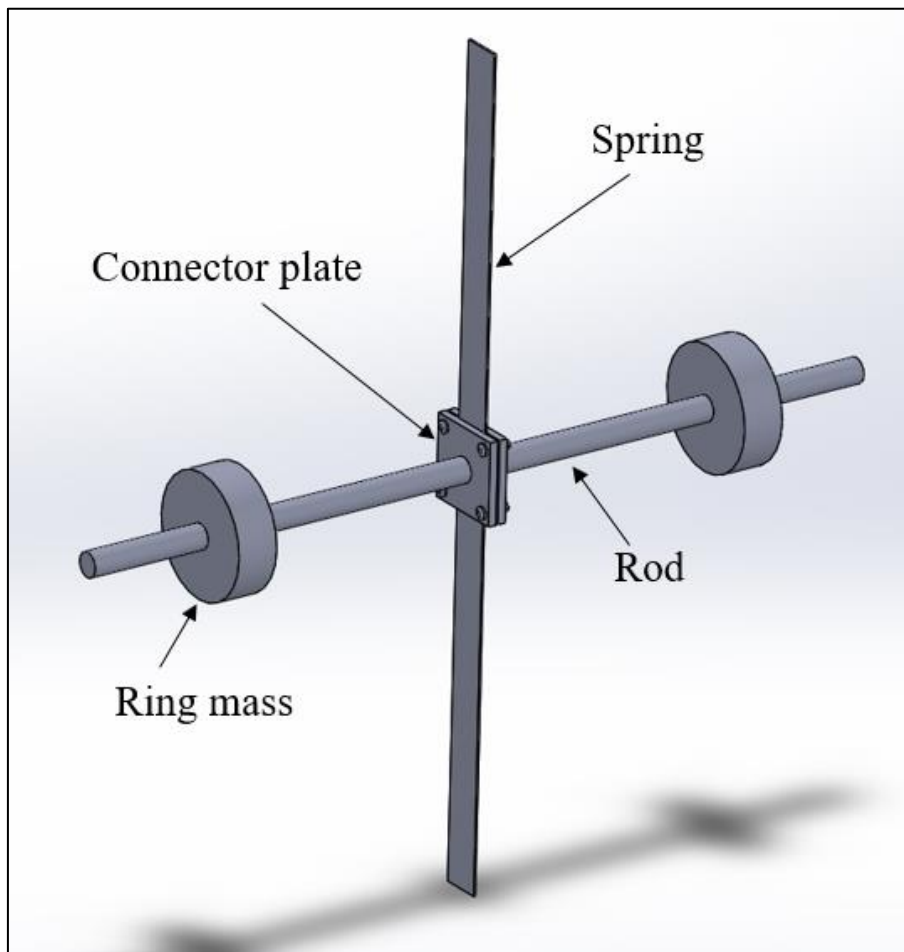
Figure 23: Torsional pendulum design with engineered external inertia

The eigen frequencies obtained are found in Table 16,

Table 16: Eigenfrequencies obtained using the parallel axis theorem

Distance R (mm)	Frequency f (Hz)	R^2 (mm^2)	T^2 (s^2)
5	5.4765	380.25	0.033342
20	5.2083	1190.25	0.036864
40	4.6051	2970.25	0.047154
60	4.0936	5550.25	0.059675
80	3.559	8930.25	0.078949
100	3.1457	13110.25	0.101057
120	2.7904	18090.25	0.12843
140	2.507	23870.25	0.159108
160	2.2653	30450.25	0.194872
180	2.0665	37830.25	0.234169

The linearity of T^2 versus R^2 proves the parallel axis theorem.
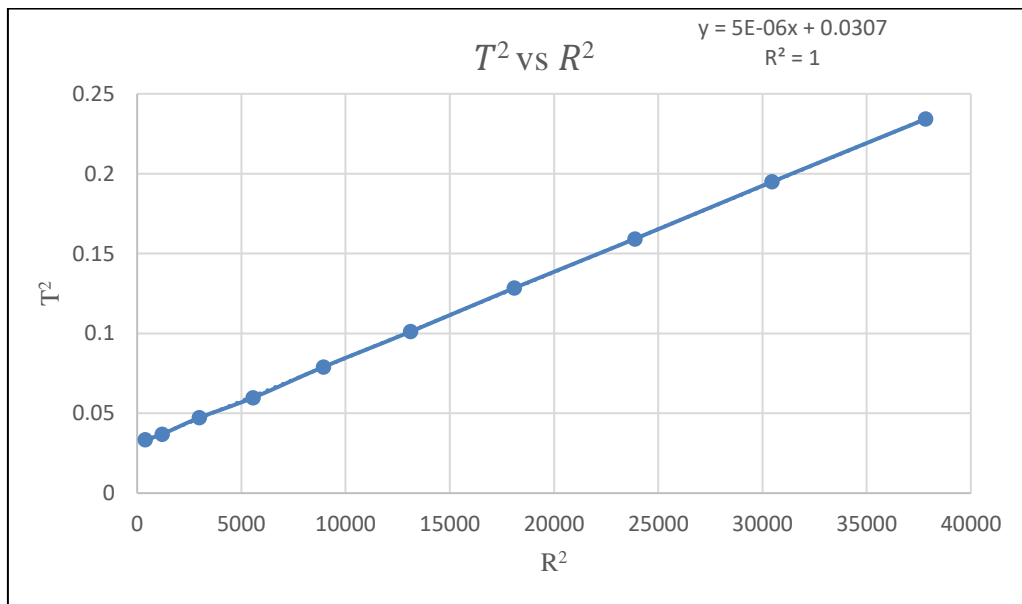
Figure 24: Verification of the parallel axis theorem

To find the shear modulus, total inertia and the value for constant z is calculated.

$$\omega_0 = \frac{2\pi}{T} = \sqrt{\frac{G\beta w t^3 z}{L_{eff} I_{ext}}} \qquad (19)$$

$$T^2 = (2\pi)^2 \times \frac{L_{eff} I_{ext}}{G\beta w t^3 z} \qquad (33)$$

Linearizing the equation gives the slope k,

$$y = kx + c \qquad (26)$$

$$y = T^2, \qquad x = I_{ext}, \qquad k = (2\pi)^2 \times \frac{L_{eff}}{G\beta w t^3 z}, \qquad c = 0$$

$$T^2 = k I_{ext} + 0 \qquad (34)$$

$$slope = k = (2\pi)^2 \times \frac{L_{eff}}{G\beta w t^3 z} \qquad (35)$$

The equation to find z will be,

$$z = (2\pi)^2 \times \frac{L_{eff}}{G\beta w t^3 k} \qquad (36)$$

The mass moment of inertia of the system could also be obtained using SolidWorks as it provides in different axes. To figure out the correct mass moment of inertia, the axis of rotation must be determined. Thus, the mass moment of inertia is calculated manually. Total inertia will include the inertia of the spring, connector plates, rods and the ring masses.

Table 17: Mass moment of inertia of the components of the torsional pendulum

Property	Equation
Mass moment of Inertia of the spring	$I = \dfrac{1}{12}m(w^2 + t^2)$
Mass moment of Inertia of the plates	$I = 2 \times \dfrac{1}{12}m(w^2 + t^2) + m(\dfrac{t_{plate}}{2} + \dfrac{t_{spring}}{2})^2$
Mass moment of Inertia of the rods	$I = 2 \times \left[\dfrac{1}{12} \times ml^2 + m\left(\dfrac{l_{rod}}{2} + \dfrac{t_{spring}}{2} + t_{plate}\right)^2\right]$
Mass moment of Inertia of the ring masses	$I = 2mr^2$

4.3.1 Mass moment Inertia I of the spring
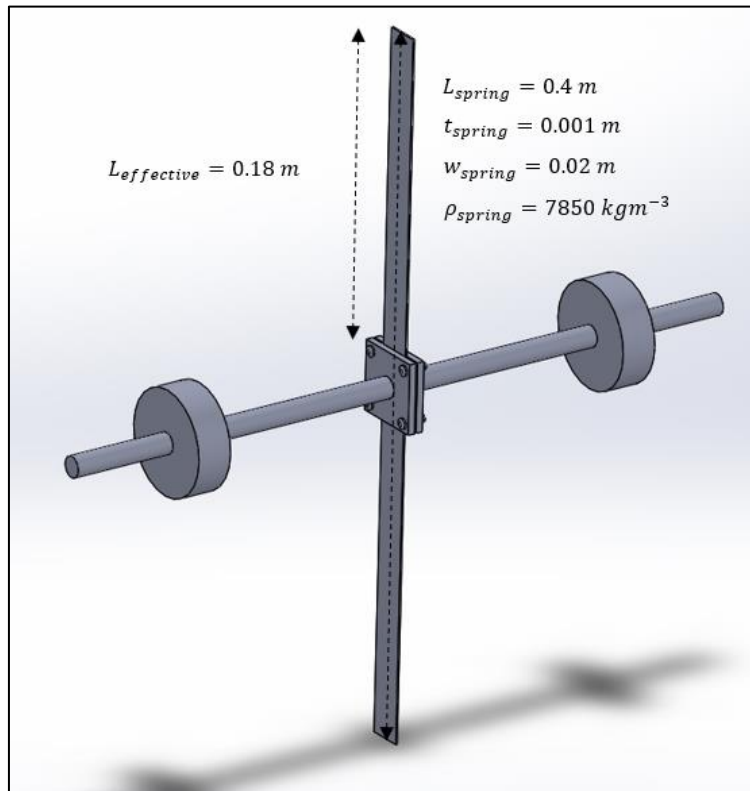
Figure 25: Mass moment inertia of the spring

The spring is located on the axis of rotation. Thus, the mass moment of inertia is calculated simply using the equation for a rectangle.

$$I = \frac{1}{12}m(w^2 + t^2) \qquad (37)$$

$$w = width\ of\ the\ spring = 0.02\ m$$

$$t = thickness\ of\ the\ spring = 0.001\ m$$

$$L = Length\ of\ the\ spring = 0.4\ m$$

$$\rho = density\ of\ the\ spring = 7850\ kgm^{-3}$$

$$m = mass\ of\ the\ spring = \rho wtL = 0.02\ m \times 0.001\ m \times 0.4\ m \times 7850\ kgm^{-3}$$

$$= 0.0628\ kg$$

$$I_{spring} = \frac{1}{12} \times 0.0628\ kg \times [(0.02\ m)^2 + (0.001\ m)^2] = \boldsymbol{2.09857 \times 10^{-6}\ kgm^2}$$

4.3.2 Mass moment Inertia I of the connector plates

$t_{plate} = 0.004\ m$

$w_{plate} = 0.04\ m$

$L_{plate} = 0.04\ m$

$\rho_{plate} = 7850\ kgm^{-3}$
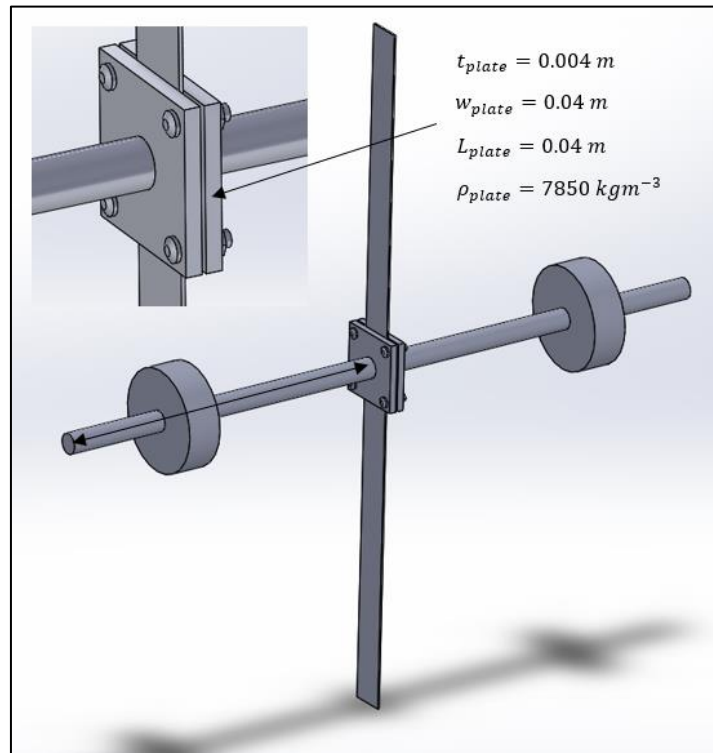
Figure 26: Mass moment inertia of the connector plates

The mass moment inertia of the connector plate is calculated using the parallel axis theorem as the centroid of the plate is not on the axis of rotation. It is displaced by half the thickness of the spring plus half the thickness of the connector plate itself.

$$I = 2 \times \frac{1}{12}m(w^2 + t^2) + m(\frac{t_{plate}}{2} + \frac{t_{spring}}{2})^2 \tag{38}$$

$$w = width\ of\ the\ plate = 0.04\ m$$

$$t = thickness\ of\ the\ plate = 0.004\ m$$

$$L = Length\ of\ the\ plate = 0.04\ m$$

$$\rho = density\ of\ the\ plate = 7850\ kgm^{-3}$$

$$m = mass\ of\ the\ plate = \rho wtL = 0.04\ m \times 0.004\ m \times 0.04\ m \times 7850\ kgm^{-3}$$

$$= 0.05024\ kg$$

$$I_{plate} = 2 \times \frac{1}{12} \times 0.05024\ kg \times [(0.04\ m)^2 + (0.004\ m)^2]$$

$$+ 0.05024\ kg \times \left(\frac{0.004\ m}{2} + \frac{0.001\ m}{2}\right)^2 = \mathbf{1.4159 \times 10^{-5}\ kgm^2}$$

49

4.3.3 Mass moment Inertia I of the rods

$l_{rod} = 0.2\ m$

$r_{rod} = 0.006\ m$

$\rho_{rod} = 7850\ kgm^{-3}$
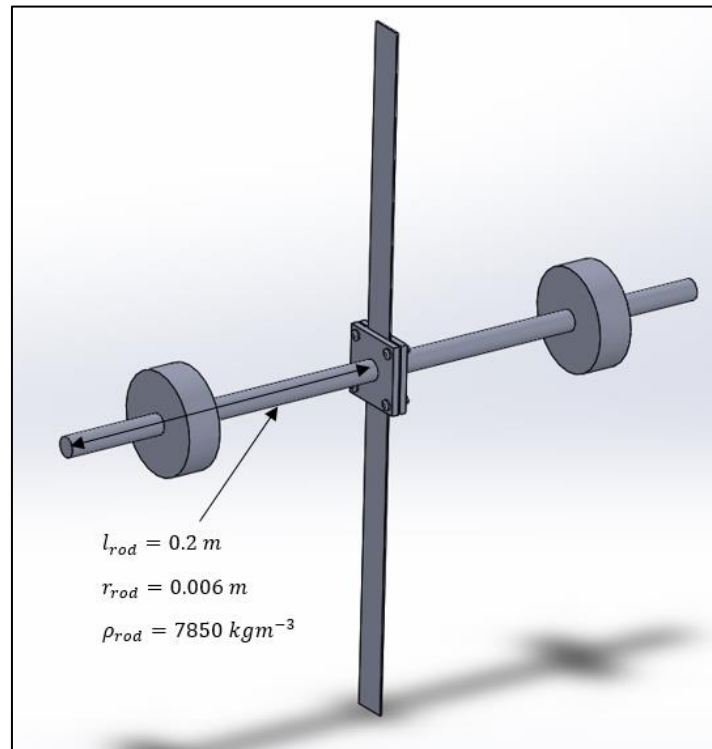
Figure 27: Mass moment inertia of the rods

The mass moment inertia of the rod is calculated using the parallel axis theorem as the centroid of the rod is not on the axis of rotation. It is displaced by half the thickness of the spring, thickness of the connector plate plus half the thickness of the rod itself.

$$I = 2 \times \left[\frac{1}{12} \times ml^2 + m \left(\frac{l_{rod}}{2} + \frac{t_{spring}}{2} + t_{plate} \right)^2 \right] \tag{39}$$

$$l = Length\ of\ the\ rod = 0.2\ m$$

$$r = radius\ of\ the\ rod = 0.006\ m$$

$$\rho = density\ of\ the\ rod = 7850\ kgm^{-3}$$

$$m = mass\ of\ the\ rod = \rho\pi r^2 l = 7850\ kgm^{-3} \times \pi \times (0.006\ m)^2 \times 0.2\ m$$

$$= 0.1776\ kg$$

$$I_{rod} = I = 2 \times \left[\frac{1}{12} \times 0.1776\ kg \times (0.2\ m)^2 + 0.1776\ kg \times \left(\frac{0.2\ m}{2} + \frac{0.001\ m}{2} + \frac{0.004\ m}{2} \right)^2 \right]$$

$$= \boldsymbol{0.004914\ kgm^2}$$

4.3.4 Mass moment Inertia I of the ring masses
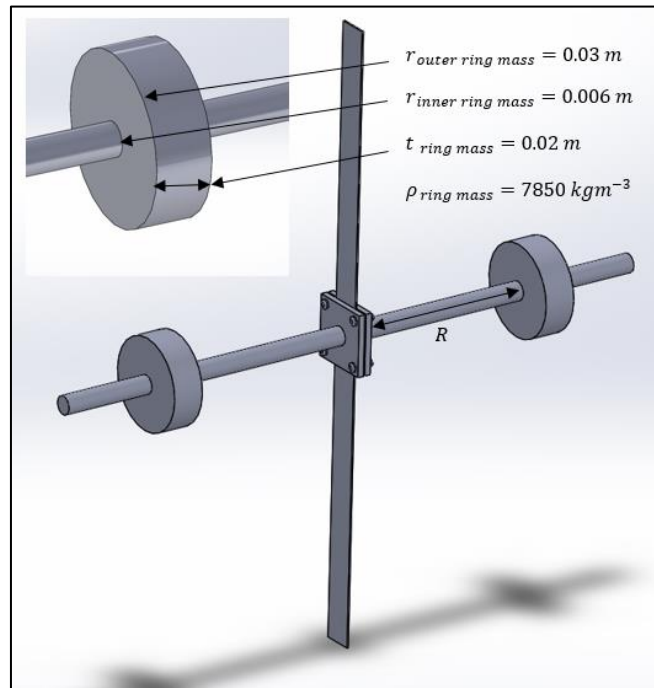
Figure 28: Mass moment inertia of the ring masses

The mass moment of inertia of the ring masses were calculated using the effective distance R_{eff} according to the distance R from the midpoint of the spring. Effective distance is the distance between the ring mass and the connector plate, thickness of the plate, half the thickness of the spring and the ring mass.

$$I = 2mR_{eff}^2 \qquad (40)$$

$$t = thickness\ of\ the\ ring\ mass = 0.02\ m$$

$$\rho = density\ of\ the\ ring\ mass = 7850\ kgm^{-3}$$

$$m = mass\ of\ the\ ring\ mass = \rho t \pi [(r_{outer})^2 - (r_{inner})^2]$$

$$m = 7850\ kgm^{-3} \times 0.02\ m \times \pi \times [(0.03\ m)^2 - (0.006\ m)^2]$$

$$m = 0.4262\ kg$$

$$R_{eff} = effective\ distance = R + \frac{t_{spring}}{2} + t_{plate} + \frac{t_{ring\ mass}}{2}$$

$$R_{eff} = 0.005\ m + \frac{0.001\ m}{2} + 0.004\ m + \frac{0.02\ m}{2} = 0.0195\ m$$

$$I = mR_{eff}^2$$

$$I = 2 \times 0.4262\ kg \times (0.0195\ m)^2 = \mathbf{0.000324\ kgm^2}$$

The total mass moment of inertia I was calculated by placing the external inertia at certain distance R.

Table 18: Total mass moment of inertia of the torsional pendulum

Distance R (mm)	Total mass moment of inertia I (kgm^2)	T^2 (s^2)
5	0.005400782	0.033342
20	0.006091146	0.036864
40	0.007608243	0.047154
60	0.00980718	0.059675
80	0.01268796	0.078949
100	0.01625058	0.101057
120	0.020495042	0.12843
140	0.025421344	0.159108
160	0.031029488	0.194872
180	0.037319474	0.234169

The values for total mass moment of inertia I were plotted against T^2. This gives a linear relationship between the two properties. The slope of the line is the k value i.e. 6.314.
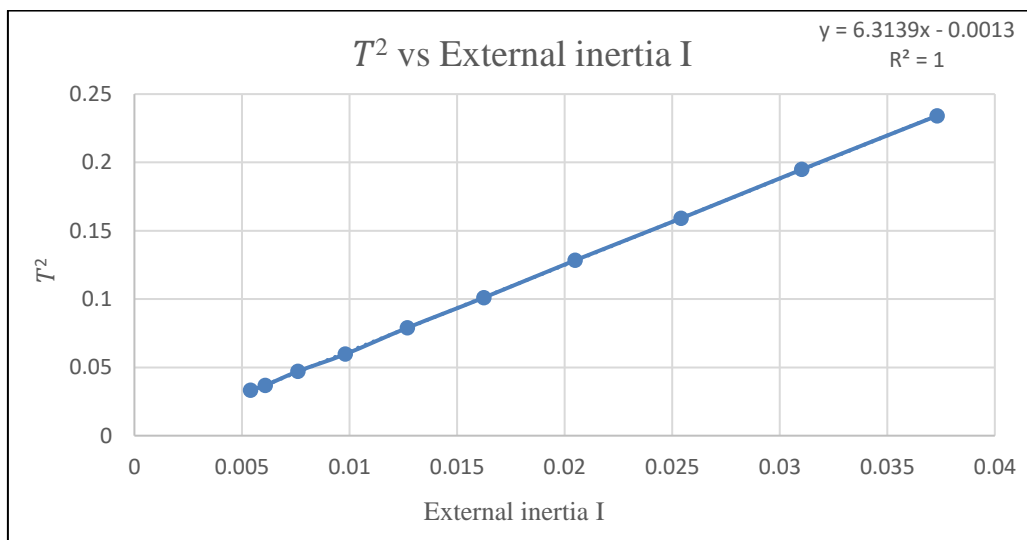
Figure 29: Relationship between the external inertia and the time squared

The slope k of the graph I plotted against T^2 is used to find the value of coupling parameter z.

$$z = (2\pi)^2 \times \frac{L_{eff}}{G'\beta wt^3 k} \qquad (36)$$

$$z = (2\pi)^2 \times \frac{3 \times 0.18\ m}{80.07\ GPa\ \times 0.02\ m \times (0.001\ m)^3 \times 6.314}$$

$$\boldsymbol{z = 2.10820047}$$

The value of coupling parameter z is 2.108. The value 2 means that the system contains two parallel springs of an effective length L_{eff}. The slight increase is due to the shortening of the lengths of the springs upon twisting. This results in the increase in stiffness. This value is inserted in the following equation to find the shear modulus of the spring.

$$G = (2\pi f)^2 \times \frac{L_{eff}\ I_{ext}}{z\beta wt^3} \qquad (41)$$

where,

$G = obtained\ shear\ modulus\ (GPa)$

$G' = Shear\ modulus\ of\ steel\ (GPa)$

$f = frequency\ (Hz)$

$L_{eff} = effective\ length\ of\ one\ spring\ (m) = \frac{(L_{spring}-L_{plate})}{2}$

$L_{eff} = (0.4\ m - 0.04\ m) \times 0.5 = 0.18\ m$

$I_{ext} = external\ mass\ moment\ of\ inertia\ (kgm^2)$

$w = width\ of\ the\ spring\ (m) = 0.02$

$t = thickness\ of\ the\ spring\ (m) = 0.001$

$\beta = ratio\ of\ width\ to\ thickness = \frac{w}{t} = \frac{0.02\ m}{0.001\ m} = 20\ \therefore \beta = \frac{1}{3}$

$z = coupling\ parameter = 2.108$

Using the equation, the values for shear modulus with external inertia at certain distance is obtained using the constant z.

Table 19: Comparison of obtained and tabulated shear modulus of the steel

Distance R (mm)	Obtained Shear modulus G (Pa)	Shear modulus G´ of Steel AISI 4340 (Pa)	Error %
5	8.19E+10	8.01E+10	2.299
20	8.36E+10	8.01E+10	4.349
40	8.16E+10	8.01E+10	1.892
60	8.31E+10	8.01E+10	3.780
80	8.13E+10	8.01E+10	1.483
100	8.13E+10	8.01E+10	1.540
120	8.07E+10	8.01E+10	0.765
140	8.08E+10	8.01E+10	0.885
160	8.05E+10	8.01E+10	0.541
180	8.06E+10	8.01E+10	0.628

Based up on the results, the constant z obtained from FEA i.e. 2.108 gave the value of shear modulus with an error not greater than 5%. This must be considered that the error increases with increasing frequency. The lower frequencies gave shear modulus with an error not greater than 1.5%. The lower frequencies were obtained when the mass rings were placed at a greater distance from the spring. Thus, giving more precise shear modulus.

4.4 Verification of COMSOL results for different materials and geometric properties

To verify that the value of the constant z obtained is the same for different cases, three different studies were conducted in COMSOL.

1. Using different materials
2. Using different lengths of the spring
3. Using different torsion constant

4.4.1 Different materials for the Spring and the Inertias

4.4.1.1 Aluminum spring

The material given to the spring was Aluminum with a density of 2700 kgm^{-3} and the material given to the external inertia was Steel AISI 4340 with a density of 7850 kgm^{-3}. The eigenfrequency study was conducted in COMSOL.

Table 20: Eigenfrequencies obtained using the parallel axis theorem for Al spring

Distance R (mm)	Frequency f of Al spring (Hz)	R^2 (mm^2)	T^2 (s^2)
5	3.1536	380.25	0.100551
20	2.9753	1190.25	0.112964
40	2.6384	2970.25	0.143654
60	2.3212	5550.25	0.185599
80	2.0385	8930.25	0.240646
100	1.8006	13110.25	0.308436
120	1.6033	18090.25	0.389019
140	1.4387	23870.25	0.483125
160	1.3018	30450.25	0.590081
180	1.1885	37830.25	0.707948

The graph for T^2 versus R^2 show the linear relationship.

55

Figure 30: Verification of the parallel axis theorem for Al spring

Total mass moment of inertia I was calculated and plotted against T^2.

Table 21: Total mass moment of inertia of the torsional pendulum with Al spring

Distance R (mm)	Total mass moment of inertia I (kgm^2)	T^2 (s^2)
5	0.005400782	0.100551091
20	0.006091146	0.112963587
40	0.007608243	0.143654331
60	0.00980718	0.185598677
80	0.01268796	0.240645956
100	0.01625058	0.308436317
120	0.020495042	0.389018643
140	0.025421344	0.483125002
160	0.031029488	0.590080775
180	0.037319474	0.707948438

The constant z value 2.108 was used to find the shear modulus.

$$G = (2\pi f)^2 \times \frac{L_{eff}\, I_{ext}}{z\beta wt^3} \qquad (41)$$

Table 22: Comparison of obtained and tabulated shear modulus of Aluminum

Distance R (mm)	Obtained Shear modulus G (Pa)	Shear modulus G´ of Aluminum (Pa)	Error %
5	2.72E+10	2.63E+10	3.258
20	2.73E+10	2.63E+10	3.661
40	2.68E+10	2.63E+10	1.817
60	2.67E+10	2.63E+10	1.584
80	2.67E+10	2.63E+10	1.361
100	2.66E+10	2.63E+10	1.288
120	2.66E+10	2.63E+10	1.282
140	2.66E+10	2.63E+10	1.157
160	2.66E+10	2.63E+10	1.093
180	2.67E+10	2.63E+10	1.342

The constant z i.e. 2.108 gave the value of shear modulus with an error not greater than 4%. The error remained below 2% with the mass rings placed at 40 mm till 180 mm.

4.4.1.2 Steel AISI 4340 spring

The material given to the spring was Steel AISI 4340 with a density of 7850 kgm^{-3} and the material given to the external inertia was Aluminum with a density of 2700 kgm^{-3}.

Table 23: Eigenfrequencies obtained using the parallel axis theorem for steel spring

Distance R (mm)	Frequency f of Steel AISI 4340 spring (Hz)	R^2 (mm^2)	T^2 (s^2)
5	9.3573	380.25	0.011421
20	8.8284	1190.25	0.01283
40	7.829	2970.25	0.016315
60	6.8875	5550.25	0.02108
80	6.0484	8930.25	0.027335
100	5.3421	13110.25	0.035041
120	4.7563	18090.25	0.044204
140	4.2676	23870.25	0.054908
160	3.8606	30450.25	0.067095
180	3.5245	37830.25	0.080502

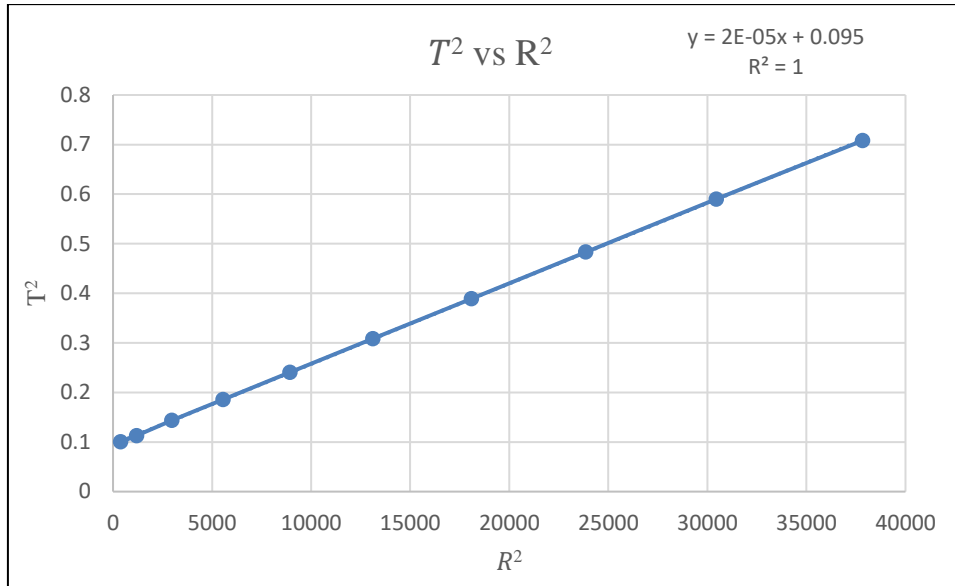The graph for T^2 versus R^2 show the linear relationship.
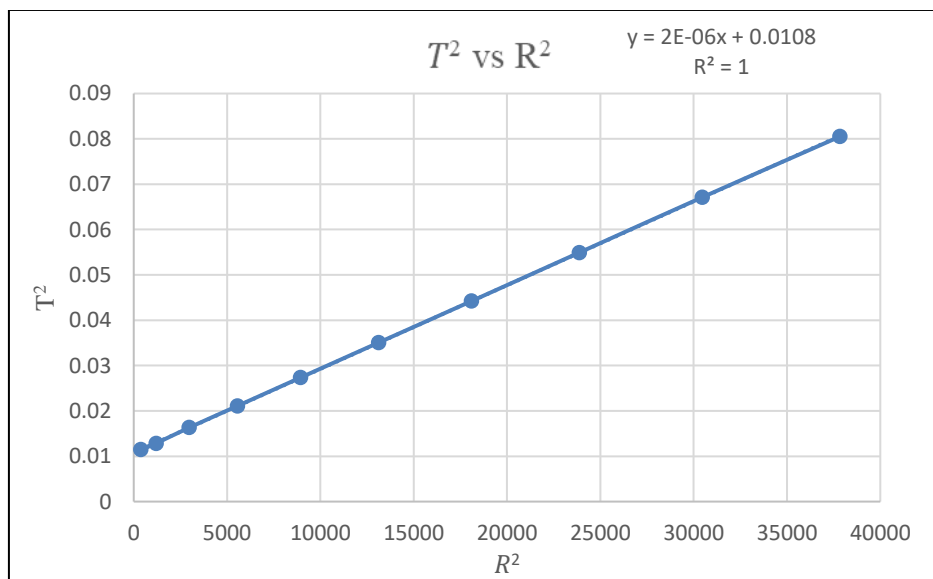
Figure 31: Verification of the parallel axis theorem for steel spring

Total mass moment of inertia I was calculated and plotted against T^2.

Table 24: Total mass moment of inertia with the steel spring

Distance R (mm)	Total mass moment of inertia I (kgm^2)	T^2 (s^2)
5	0.001859444	0.011420862
20	0.002096894	0.012830276
40	0.002618698	0.016315013
60	0.003375021	0.021080299
80	0.004365862	0.027334994
100	0.005591222	0.035040958
120	0.0070511	0.044203995
140	0.008745497	0.054907616
160	0.010674413	0.067095036
180	0.012837848	0.080501685

The constant z value 2.108 was used to find the shear modulus.

$$G = (2\pi f)^2 \times \frac{L_{eff} \, I_{ext}}{z\beta wt^3} \qquad (41)$$

Table 25: Comparison of obtained and tabulated shear modulus of the steel spring

Distance R (mm)	Obtained Shear modulus G (Pa)	Shear modulus G` Steel AISI 4340 (Pa)	Error %
5	8.23E+10	8.01E+10	2.797
20	8.26E+10	8.01E+10	3.190
40	8.12E+10	8.01E+10	1.343
60	8.09E+10	8.01E+10	1.087
80	8.08E+10	8.01E+10	0.844
100	8.07E+10	8.01E+10	0.746
120	8.07E+10	8.01E+10	0.715
140	8.05E+10	8.01E+10	0.566
160	8.04E+10	8.01E+10	0.450
180	8.06E+10	8.01E+10	0.690

The constant z i.e. 2.108 gave the value of shear modulus with an error not greater than 3.2%. The error goes below 1% if the inertia is displaced at 80 mm away from the spring.

4.4.2 Varying length L of the spring

The study was conducted by making the length L of the spring 0.2 m, 0.3 m, 0.4 m, 0.5 m, 0.7 m, 1 m and 3 m. The width was kept constant i.e. 0.02 m.
The COMSOL study for each of the lengths were conducted and the parameter z was obtained for each study.

Table 26: Coupling parameter z for different length to width ratio

Length L of the spring (m)	Ratio of length to width L/w	coupling parameter z
0.2	10	2.29195
0.3	15	2.17259
0.4	20	2.10820
0.5	25	2.08952
0.7	35	2.06984
1	50	2.04528
3	150	2.04327

The z value was plotted against the ratio of length to width.
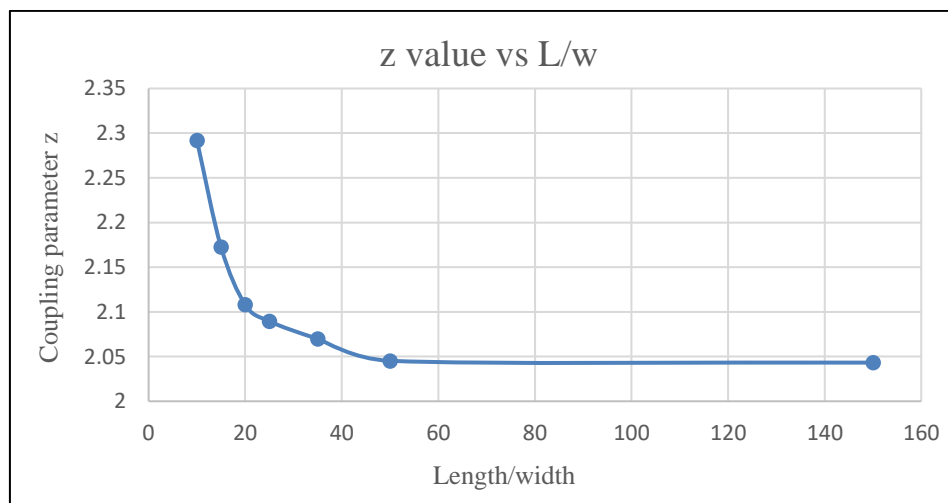
Figure 32: Relationship between the coupling parameter z and length to width ratio

As it was assumed that the system behaves like the parallel connected springs that operates simultaneously. In this case, the summing of two equal springs causes the factor of 2. The graph above proves that the results of the studies conducted in COMSOL are reliable as value for constant z is around 2. Springs are likely to contract while twisting. This shortens the length of the springs and increase the stiffness factor. That is why the value is slightly higher than 2. Even at the extreme case i.e. length of the beam is 3 m, the value of z is 2.04 and the line blends out.

If the beam is short, then the torsional motion is governed by the equation, but z is not constant.

$$\frac{L}{w} < 20 \quad z \neq constant$$

If the length to width ratio is,

$$\frac{L}{w} > 20 \quad z \approx constant$$

To use z as a constant, the beam must be made longer if the 3% error is permitted. This indicates that the beam should have a certain length for the twisting motion to be purely shear dependent. Short cantilever beams in twisting will have different shear modulus as the torsion constant J will be different.

4.4.3 Using different torsion constant

The torsion constant for a rectangular specimen is calculated using the equation as follows:

$$J = \beta a b^3 \qquad\qquad (10)$$

where,
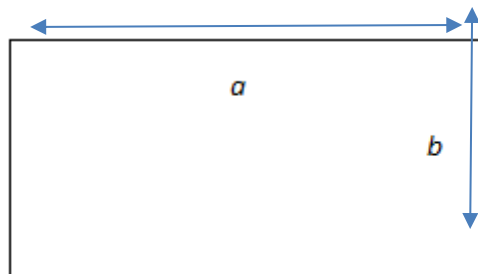
Figure 33: Schematic of showing the a and b length for the torsion constant

β value is used according to the ratio of a to b. The values for β are found in Table 27,

61

Table 27: The value for β with respect to the ratio of a to b [9]

a/b	β
1.0	0.141
1.5	0.196
2.0	0.229
2.5	0.249
3.0	0.263
4.0	0.281
5.0	0.291
6.0	0.299
10.0	0.312
∞	0.333

Previously, the width to thickness ratio was,

$$\frac{a}{b} = \frac{0.02\ m}{0.001\ m} = 20$$

So, the β value used was $\frac{1}{3}$. This study is conducted to verify if the constant z works for a different width to thickness ratio i.e. different β value.

The geometry of the spring was modified. The width was reduced by half i.e. 0.01m and thickness was kept half of the width i.e. 0.005 m.
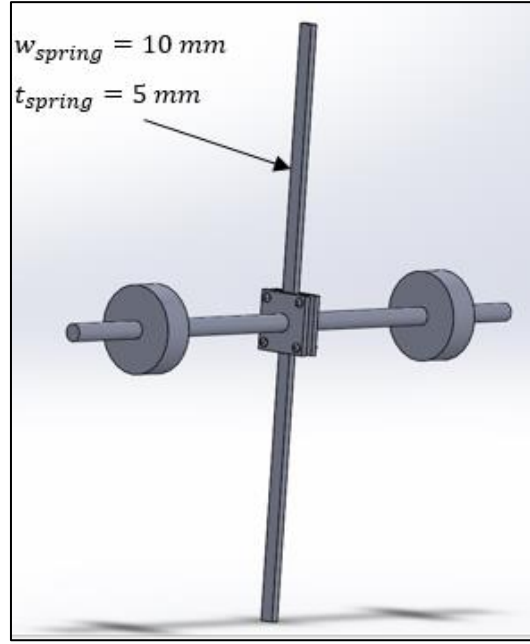
Figure 34: Design with modified spring dimensions

The width to thickness ratio the modified spring is,

$$\frac{a}{b} = \frac{0.01\ m}{0.005\ m} = 2$$

The β value for $\frac{a}{b} = 2$ is 0.229.

Table 28: Eigenfrequency and mass moment of inertia for different spring dimensions

Distance R (mm)	Frequency f (Hz)	R^2 (mm^2)	T^2 (s^2)	Total mass moment of inertia I (kgm^2)
120	18.199	18090.25	0.00302	0.021109172

$$G = (2\pi f)^2 \times \frac{L_{eff}\ I_{ext}}{\beta z w t^3} \qquad (41)$$

$$G = (2\pi \times 18.199\ Hz)^2 \times \frac{0.18\ m \times 0.021109172\ kgm^2}{0.229 \times 2.108 \times 0.01\ m \times (0.005\ m)^3}$$

$$G = 82.4 \times 10^9\ Pa$$

The constant z i.e. 2.108 and different β value gave shear modulus with an error not greater than 3%.

4.5 Verification of the coupling parameter 'z'

The coupling parameter z obtained using FEA is further verified by changing the mesh and making it "extra fine". The eigenfrequency study was conducted by increasing the length of the spring from $100\ mm$ to $500\ mm$ with a step width $dL = 10\ mm.$
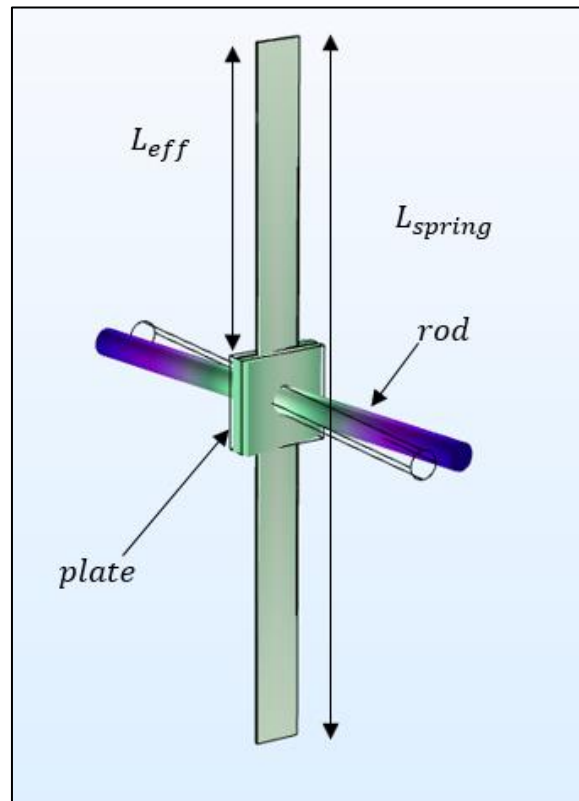
Figure 35: The design for z verification in COMSOL

Table 29 shows the dimensions of the components of the design.

Table 29: Geometric information of the design used to verify z

Parameter	Value (m)
Width of the spring	0.02
Thickness of the spring	0.001
Length of the spring	0.1 – 0.5, dL = 0.01
Length and width of the plate	0.04
Thickness of the plate	0.004
Length of one rod	0.1
Diameter of the rod	0.012

The obtained eigenfrequencies were plotted against the corresponding lengths. The graph below shows the linear relationship.
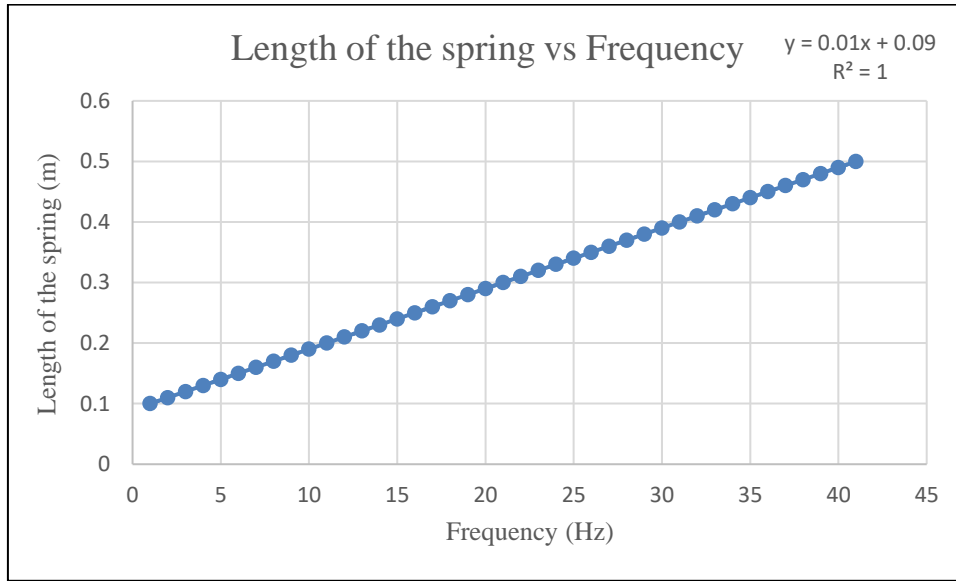
Figure 36: Relationship between frequency and the changing length of the spring

The z value describes the coupling of torsional springs. It is assumed to be around the value 2 as there are two torsional springs connected in parallel. Previously it was calculated using the parallel axis theorem for the ring masses moving along the rods. The external inertia I_{ext} was plotted against the time squared T^2 and the slope k was used to determine the value for z. In this verification the ring masses are not included. Thus, it is calculated for each spring length using the following equation,

$$\omega_0 = \frac{2\pi}{T} = \sqrt{\frac{G\beta wt^3\, z}{L_{eff}\, I_{ext}}} \tag{18}$$

$$z = \frac{(2\pi f)^2 \times L_{eff}\, I_{ext}}{G\beta wt^3} \tag{42}$$

L_{eff} = effective length of one spring (excludes the length of the connector plate)

I_{ext} = external inertia (includes the mass moment inertia of the spring, connector plates and the rods)

The graph below shows how the coupling parameter z changes according to the ratio of length to width.
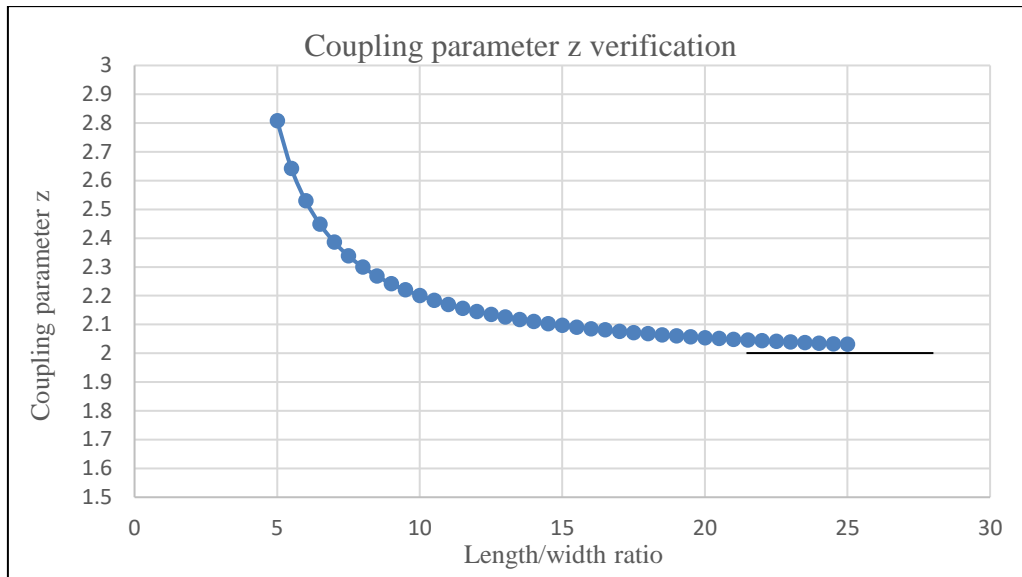
Figure 37:Verification of the z value

The graph verifies that the value for coupling parameter z does not fall below 2. The coupling function z for double clamped torsional springs can be empirically approximated by,

$$z\left(\frac{L}{w}\right) = a \left(\frac{L}{w}\right)^{b} + c \qquad (43)$$

$$z\left(\frac{L}{w}\right) = 18 \left(\frac{L}{w}\right)^{-1.95} + 2$$

valid from $\frac{L}{w} = 5 \dots 25$ with an error less than 1%.
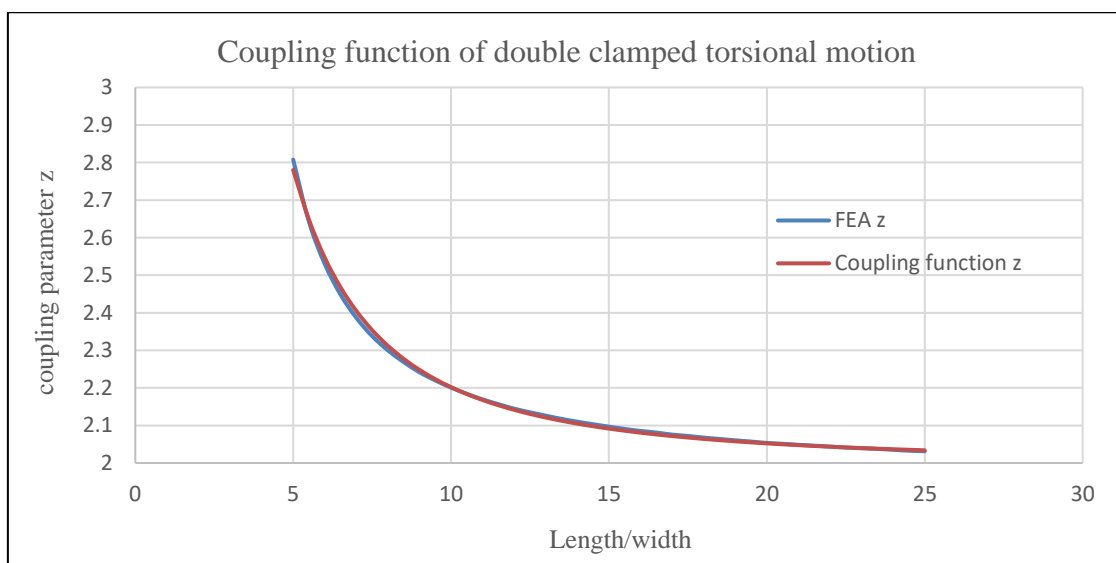
Figure 38: Coupling function of double clamped torsional motion

66

4.6 Device manufacturing and testing

4.6.1 Designing the mechanism

The mechanism needed a rigid frame that the testing specimen will be clamped to from both ends. The frame was designed in SolidWorks with respect to the manufacturability of the physical part.
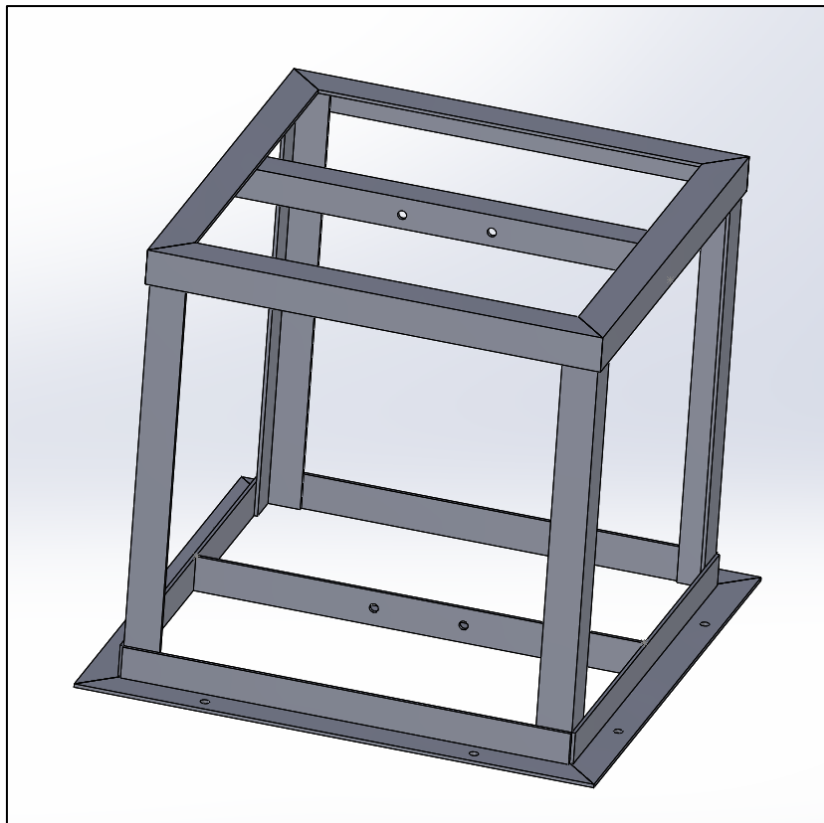
Figure 39: Design of the frame

The specimen will be clamped from both ends to the rigid frame. The height of the frame is designed based on the geometry of the design used in COMSOL analysis. The z value obtained using the COMSOL analysis was about a constant when the length to width ratio is greater than 15. The external inertia will be attached to the specimen. Figure 40 shows the representation of the original mechanism that is used in COMSOL analysis attached to the frame.
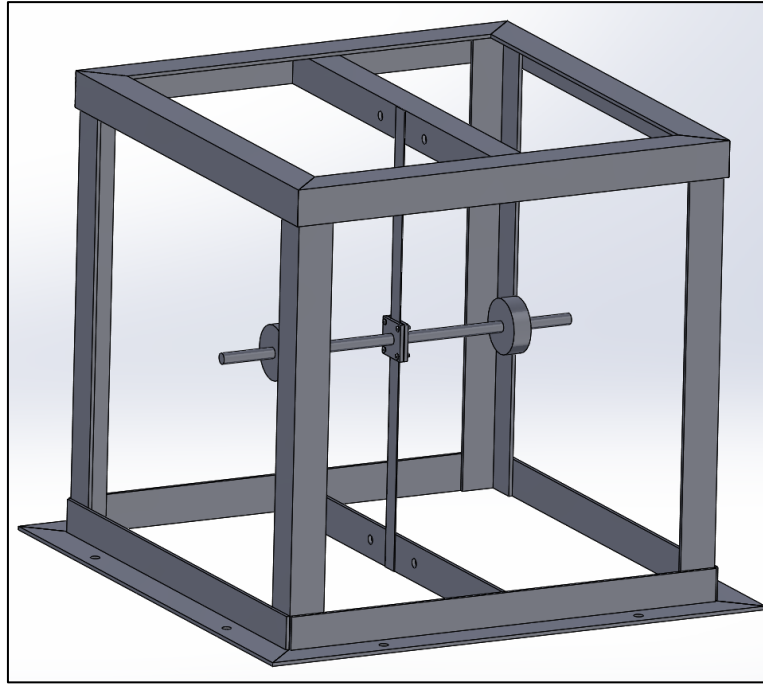
Figure 40: Assembly of the frame and the FEA torsional pendulum

The parts used as external inertia were already available for use in Arcada. The geometry of the parts was different than the original design used in FEA. So, the real part geometry was designed in SolidWorks and tested in COMSOL. The results are discussed further in section 4.6.3.
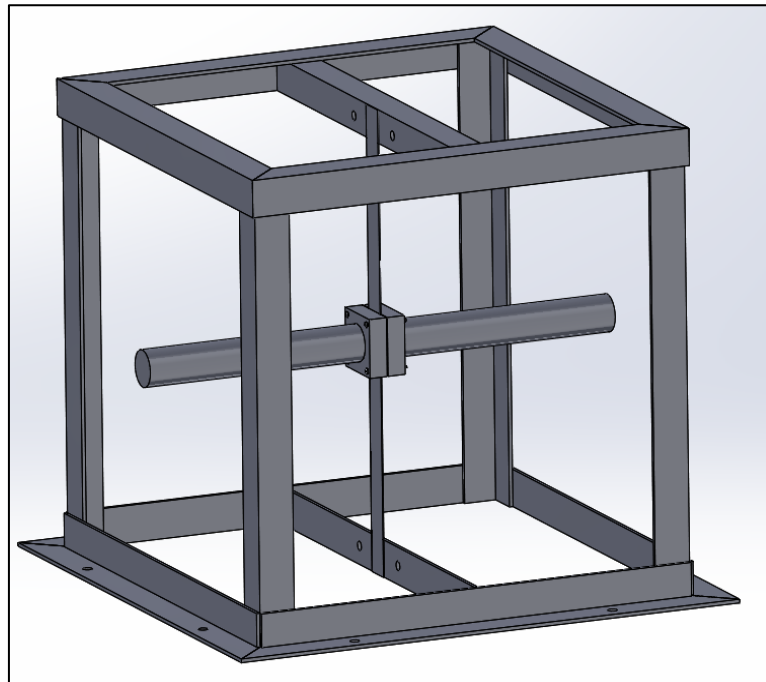
Figure 41: Design of the manufactured frame and the torsional pendulum

4.6.2 Manufacturing the mechanism

The frame was built using 40 x 40 mm steel profiles. The profiles were welded together and the holes were drilled for the screws to fix the plates against the frame. The frame was clamped to the table. The specimen will pass through the plates and the frame and clamped in between by tightening the screws.
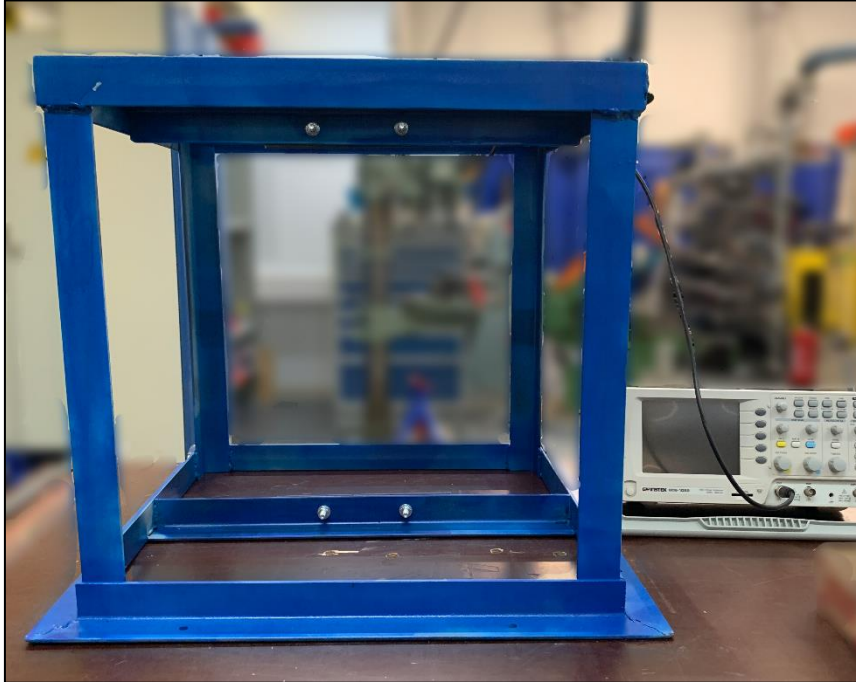
Figure 42: Manufactured frame

The external inertia was clamped in the middle of the specimen. It includes two connector plates and two rods. Two screws will keep the connector plate and the rod together. Four screws are needed to clamp the test piece.
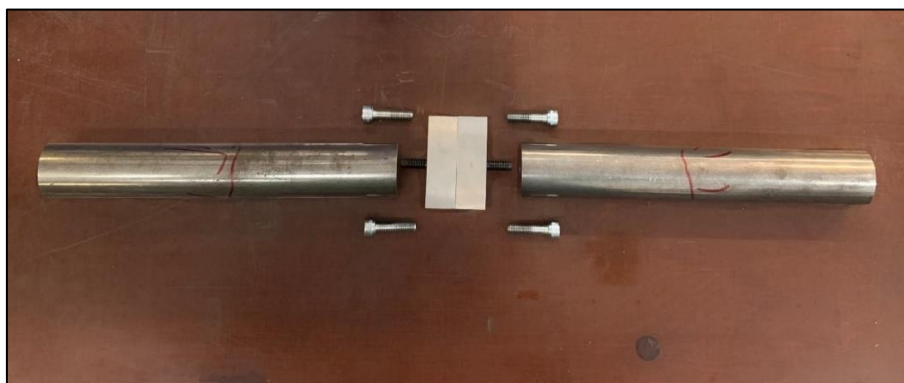
Figure 43: External inertia components

The table shows the geometry and mass of the components of external inertia.

Table 30: Physical properties of the external inertia

Parameter	Connector plate	Rod
Length (m)	0.063	0.250
Width (m)	0.063	-
Thickness (m)	0.02	-
Diameter (m)	-	0.04
Mass (kg)	0.571	2.445

Figure 44 shows the assembled mechanism. A sensor was glued on to the specimen to detect the vibrational frequency and attached to the oscilloscope. The external inertia is moved to a side and released to create vibration in the specimen. The oscilloscope provided the wave signal and frequency of the wavelength due to the vibration.
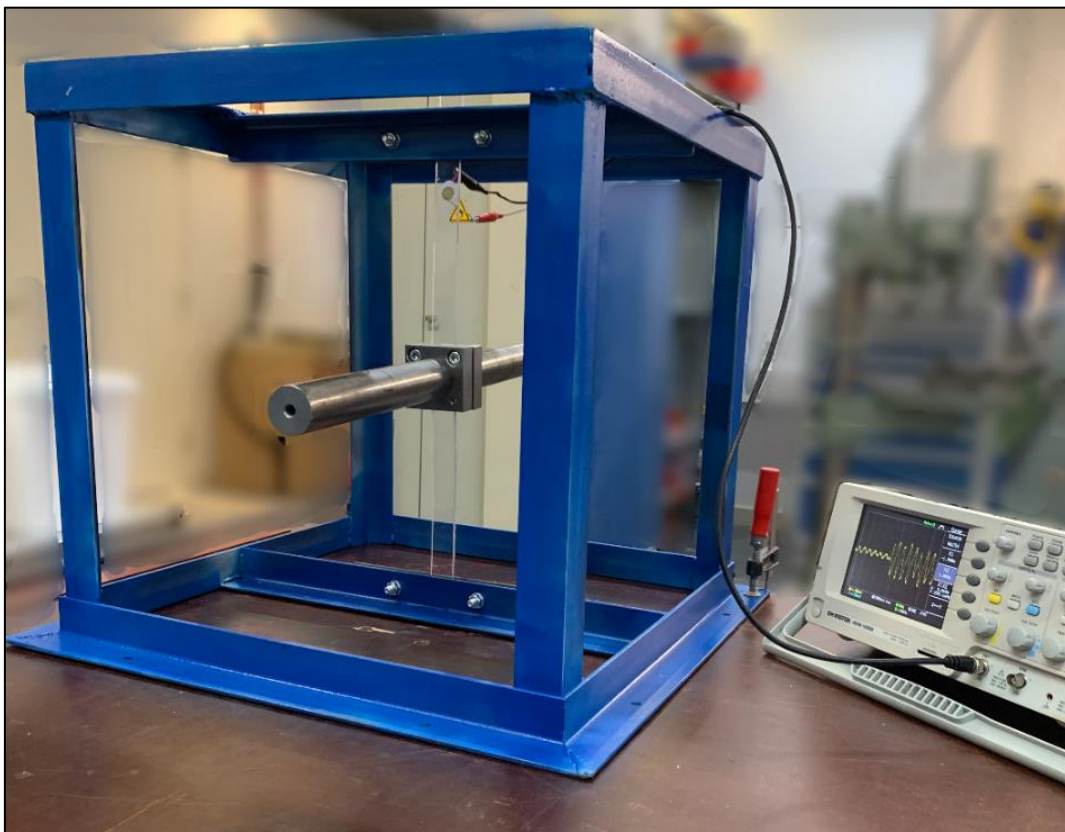
Figure 44: Assembled mechanism

The frequency of a wavelength of the signal is used to find the shear modulus of the specimen using the equation.

$$G = (2\pi f)^2 \times \frac{L_{eff}\, I_{ext}}{\beta z w t^3} \qquad (41)$$

4.6.3 Testing the mechanism

The mechanism was tested using a thin plate made of steel. The frequency was obtained using three different ways.

- Measuring the frequency using oscilloscope
- Manually by counting the number of oscillations
- Obtaining frequency using FEA

Table 31: Dynamic Shear modulus obtained using different methods

Method	Frequency (Hz)	Dynamic shear modulus (GPa)
Oscilloscope	1.389	82.46
Manual (counting oscillations)	1.418	84.97
FEA (COMSOL Multiphysics)	1.408	84.73
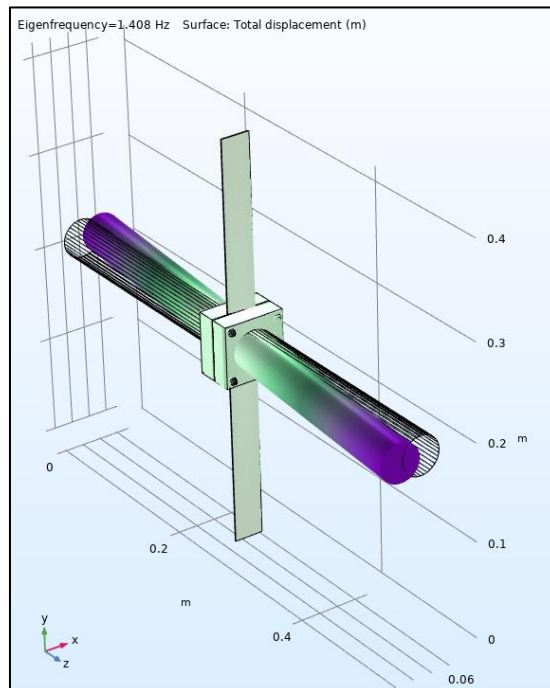
Figure 45: COMSOL simulation for the design of the actual mechanism

The frequency values obtained are about the same proving that the mechanism works in the case of thin plates. The dynamic shear modulus obtained using the frequencies is close to the tabulated shear modulus of steel. The frequency obtained using the oscilloscope gives the shear modulus with an error less than 3%.

The external inertia rods were too heavy to obtain the vibration in torsion mode only. In the case of thin plates, the specimen was going through first and second mode of bending along with torsion. This will give inaccuracy in results. To get the torsion mode only, the external inertia was halved. Thus, the length of one rod was 0.125 meters.
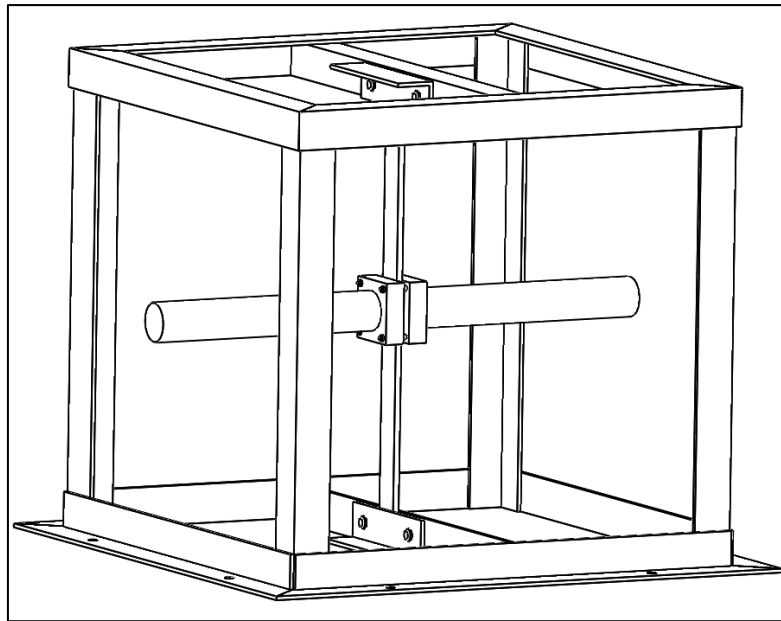
Figure 46:Schematic of the manufactured mechanism

Other than the steel, the tests were carried out on the composite specimens made of (E-glass) glass fiber and Distitron VE370 resin. The composites comprised of two different textiles, Unidirectional [0°, 90°, random angle (M70)] and Biaxial [± 45°, random angle (M100)].

Table 32: Material properties of E- glass fiber

Material Properties of (E- glass) fiber	
Young's Modulus (E)	70 GPa
Poisson number (nu)	0.25
Shear Modulus (G)	28 GPa
Density (ρ)	2540 kgm^{-3}

Table 33: Material properties of the resin

Material Properties of Distitron VE370 resin	
Young's Modulus (E)	4 GPa
Poisson number (nu)	0.35
Shear Modulus (G)	1.48 GPa
Density (ρ)	$1100 \ kgm^{-3}$

The glass fiber textile consists of three different layers arranged in 0°, 90° and random angle. Each layer has its own mass textile and thickness. Unidirectional textile comprises of,

Table 34: Mass textile per the angle in unidirectional textile

Angle (°)	Mass textile (kgm^{-2})
0	1.152
90	0.051
random (0)	0.070

The thickness of the specimen with [0°, 60°, -60°, 0°] $_{sym}$ lamina setup was measured to be 6.65 mm. The thickness and mass textile were used to find the fiber volume fraction. [20]

$$Fiber \ volume \ fraction = \frac{mass \ textile}{density \times thickness} = \frac{M_{tex}}{\rho \times t} \qquad (44)$$

$$= \frac{8 \times 1.273 \ kgm^{-2}}{2540 \ kgm^{-3} \times 0.00665 \ m} = 0.60292 \approx \mathbf{60\%}$$

The lamina setup was placed in CCSM as follows,

Table 35: Lamina layup in CCSM

Ply	Angle (°)	E11 (GPa)	E22 (GPa)	G12 (GPa)	nu12	thickness (mm)
1	0	43.6	9.210526	3.431373	0.29	0.757874
2	90	43.6	9.210526	3.431373	0.29	0.033465
3	0	9.210526	9.210526	3.431373	0.29	0.045932
4	60	43.6	9.210526	3.431373	0.29	0.757874
5	150	43.6	9.210526	3.431373	0.29	0.033465
6	0	9.210526	9.210526	3.431373	0.29	0.045932
7	-60	43.6	9.210526	3.431373	0.29	0.757874
8	30	43.6	9.210526	3.431373	0.29	0.033465
9	0	9.210526	9.210526	3.431373	0.29	0.045932
10	0	43.6	9.210526	3.431373	0.29	0.757874
11	90	43.6	9.210526	3.431373	0.29	0.033465
12	0	9.210526	9.210526	3.431373	0.29	0.045932

The total thickness obtained was $6.698\ mm$ and d_{33} is $6923.05\ MPa^{-1}m^{-3}$. The shear modulus using d_{33} from CCSM is obtained by following equation, [21]

$$E_{twist} = \frac{12}{t^3 d_{33}} \qquad (45)$$

$$= \frac{12}{(0.006698\ m)^3 \times (6923.05 \times 10^3)\ GPa^{-1}m^{-3}} = \boldsymbol{5.77\ GPa}$$

The lamina setup was placed in CCSM and shear modulus was obtained. This shear modulus was compared to the dynamic shear modulus obtained by placing the specimen in the mechanism and made it to vibrate. Table 36 shows the other parameters along with the frequency obtained from oscilloscope, that are needed to find the shear modulus.

Table 36: Parameters and the values to find the dynamic shear modulus

f	Frequency (Hz)	15.06
L_{eff}	Effective length of one spring (m)	0.176
I_{ext}	External Inertia of spring, plates, rods (kgm^2)	0.022
w	width of the spring (m)	0.034
t	thickness of the spring (m)	0.00665
β	$\dfrac{w}{t} > 5$	0.291
z	coupling parameter	2.108

The parameters above were inserted in the following equation:

$$G = (2\pi f)^2 \times \frac{L_{eff}\, I_{ext}}{\beta w t^3 z} \qquad (41)$$

$$G = (2\pi \times 15.06\ Hz)^2 \times \frac{0.176\ m \times 0.022\ kgm^2}{0.291 \times 0.034\ m \times (0.00665\ m)^3 \times 2.108} = 5.657\ GPa$$

Table 37 shows the comparison of the results obtained from the CCSM and the experiment.

Table 37: Comparison of the results obtained using the mechanism and CCSM

Method	Result
G (CCSM)	5.77 GPa
G (Test)	5.657 GPa
Relative Error	1.93%

The dynamic shear modulus obtained from the material testing gives the result with an error less than 2% compared to the shear modulus obtained using the CCSM.

More samples with different layup were tested and verified by comparing them with CCSM results.

Table 38: Verification of the mechanism by testing more samples

Lamina setup	Thickness (mm)	Frequency (Hz)	(CCSM) (GPa)	(Test) (GPa)	relative error	error %
$[0°, +30°, -30°, 0°]_{sym}$	6.6	16.03	5.873	6.377	-0.0859	8.588
$[0°, +60°, -60°, 0°]_{sym}$	6.65	15.06	5.768	5.657	0.0193	1.932
$[+45°, -45°, 0°, +45°, -45°]_{sym}$	4	8.264	7.294	7.263	0.0043	0.426

The results obtained are relatively similar. The difference in results is due to many reasons. The specimens used for testing are laminated composites. There is a variation in the thickness of the specimen. The fiber volume fraction is obtained using the thickness of the specimen which leads to the input values in CCSM. Also, the mechanism is in its early stage of development. The slight inaccuracy could also be due to the frame not being fixed from all sides, loose clamping of the specimen from both ends and the external inertia not being clamped exactly in the middle due to personal error.

5 DISCUSSION

This study is based on a standard that does not depend on analytical derivation, whereas it depends on experimental findings. Finite Element Analysis was used to validate the mechanism built to measure the dynamic shear modulus.

The hypothesis that the coupling parameter 'z' will be slightly greater than 2 is proved to be correct. For it to be about a constant, the spring must be long enough i.e. the length to width ratio should be greater than 20.

After successfully obtaining the value for parameter z, the point of consideration was if the interface between the external inertia and the spring will limit the numeric accuracy. The sharp edge between the spring and the external inertia will affect the meshing and give inaccurate results. For verification, the mesh size was changed to extra fine and extremely fine to see if there is a big variation. The eigenfrequencies obtained using different mesh sizes did not vary a lot. In addition to this the value for coupling parameter 'z' was calculated using the FEA results for eigenfrequencies obtained by creating extra fine mesh and using lengths of the spring from 100 mm to 500 mm with a step width of 10 mm. The value did not go below 2. This proves that the FEA is a reliable method for this study and gives trustworthy results.

The mechanism built in the later stage is still not fully developed. It allowed to test if the experimental results correspond to the FEA results. The mechanism must be assembled and dissembled every time a new specimen is to be tested. The sensors are to be glued on to every test specimen. The frame is clamped from one side, but it should be fixed from all sides, so that it does not move. The stiffness of the frame could also be increased by adding diagonal stiffeners.

The mechanism could be made better by clamping another external inertia to the specimen. By moving both the masses in opposite directions will eliminate the net torque on the frame. This modified mechanism will also provide more information, such as the bending modulus of the test specimen.

6 CONCLUSION

The approach for obtaining the dynamic shear modulus of fixed-fixed thin plates using a torsional pendulum has been successfully achieved. Dynamic testing method is a better alternative to obtain shear modulus of a specimen as the static testing method for shear test would be much expensive. In addition, this is a non-destructive testing method and experimentally dynamic shear modulus is obtained by means of a torsional pendulum. If the specimen was clamped on one end, then the signal will be distorted by the other modes of vibration that will be existing simultaneously. To suppress the other modes, the specimen was clamped on both ends. The study is based on the existing standard ASTM E1876-15. Since, the standard is not based on any analytical derivation, Finite Element Analysis was used to prove the results. A rectangular plate with an external inertia was designed in SolidWorks and using COMSOL Multiphysics 5.4, eigenfrequency study was conducted by clamping the specimen at both ends.

One of the aims was to obtain a boundary condition for the coupling parameter z to be constant. It is expected to be larger than 2 as there are two springs connected in parallel. The slight increase in the value would be due to the simultaneous contraction while twisting, resulting in the increase in stiffness. The value for the coupling parameter z was obtained to be greater than 2 using equation 42.

$$z = \frac{(2\pi f)^2 \times L_{eff} \, I_{ext}}{G\beta wt^3}$$

The positive side effect of this study compared to the existing standard ASTM E1876-15, is the addition of external inertia to lower the frequency and make the viscous damping insignificant. Equation 41 was used to calculate the dynamic shear modulus.

$$G = (2\pi f)^2 \times \frac{L_{eff} \, I_{ext}}{z\beta wt^3}$$

The dynamic shear modulus obtained using FEA and the coupling parameter z was obtained with an error less than 5 %.

As the external inertia was moved further away from the specimen, the error decreased to less than 1 %. The study was verified by varying the length of the spring, using different materials and torsion constant.

The coupling parameter z was verified by making the mesh size extra fine. The study was conducted for the spring length from 100 mm to 500 mm with a step width of 10 mm.

The coupling function z was empirically approximated as expressed in equation 43.

$$z\left(\frac{L}{w}\right) = 18\left(\frac{L}{w}\right)^{-1.95} + 2$$

The mechanism was designed and manufactured. It was tested using the same specimen specifications used in FEA. The dynamic shear modulus using the mechanism was obtained with an error less than 3 %.

7 REFERENCES

[1] M. Ciccotti and F. Mulargia, "Differences between static and dynamic elastic moduli of a typical seismogenic rock," *Geophysical Journal International,* vol. 157, no. 1, pp. 474-477, 2004.

[2] "E-Labs," E-Labs Inc., 2019. [Online]. Available: http://www.e-labsinc.com/dynamics-testing.shtml. [Accessed 15 01 2020].

[3] M. A. Meyers and K. K. Chawla, "Plasticity," in *Mechanical Behavior of Materials*, Cambridge University Press, 2009, p. 162.

[4] B. Bollen, "The Impulse Excitation technique, an innovative NDT method for microstructure and mechanical properties characterization of refractory materials used in the aluminum industry.," AMAP, 2016.

[5] IMCE, "Theory," IMCE, 2020. [Online]. Available: imce.eu/theory. [Accessed 15 01 2020].

[6] E. BRITTANICA, "Shear Modulus," Encyclopædia Britannica, Inc., 2019. [Online]. Available: https://www.britannica.com/science/shear-modulus. [Accessed 17 10 2019].

[7] R. Hibbeler, Mechanics of Materials, Pearson, 2014.

[8] Z. Nakhoda and K. Taylor, "Effective Torsion and Spring Constants in a Hybrid Translational Rotational Oscillator," *THE PHYSICS TEACHER,* vol. 49, February 2011.

[9] "Torsion constant," Wikipedia, 26 09 2019. [Online]. Available: https://en.wikipedia.org/wiki/Torsion_constant#cite_note-8. [Accessed 16 01 2020].

[10] S. K. Fenster, A. C. Ugural and A. C. Ugural, Advanced Strength and Applied Elasticity, Elsevier Publishing Company, 1975.

[11] "Mass Moment of Inertia," The Engineering ToolBox, [Online]. Available: https://www.engineeringtoolbox.com/moment-inertia-torque-d_913.html. [Accessed 16 01 2020].

[12] "University Physics Volume 1," OpenStax , Houston, 2020.

[13] "Hooke's Law," Wikipedia, 16 01 2020. [Online]. Available: https://en.wikipedia.org/wiki/Hooke%27s_law. [Accessed 17 01 2020].

[14] M. Kervinen, I. Parkkila and P. Konttinen, MAOL taulukot, Keuruu: MAOL ry ja Kustannusosakeyhiö Otava, 2015.

[15] "FEA," Simscale, [Online]. Available: https://www.simscale.com/docs/content/simwiki/fea/whatisfea.html. [Accessed 17 01 2020].

[16] "Eigenfrequency Analysis," COMSOL, 08 05 2018. [Online]. Available: https://www.comsol.com/multiphysics/eigenfrequency-analysis. [Accessed 17 01 2020].

[17] H. Sönnerlind, "How to Analyze Eigenfrequencies That Change with Temperature," COMSOL Blog, 2017.

[18] G. Staab, "Lamina Analysis," in *Laminar Composites*, Butterworth-Heinemann, 2015, p. 83.

[19] G. Staab, "Lamina Analysis," in *Laminar Composites*, Butterworth-Heinemann, 2015, p. 70.

[20] "Composites Design and Manufacture," ACMC, 2019. [Online]. Available: https://www.fose1.plymouth.ac.uk/sme/MATS347/MATS347A1%20basics.htm. [Accessed 06 03 2020].

[21] G. Staab, "Laminate Anlaysis," in *Laminar Composites*, Butterworth-Heinemann, 2015, p. 200.

8 APPENDIX

Item	Quantity	Description (mm)	Length (mm)
1	4	40x40x4	580
2	4	40x40x4	508
3	4	40x40x4	500
4	2	40x40x4	500
5	14	R5	

	NAME		TITLE: **Steel frame**	
DRAWN	Saara Ishfaq			
			DWG NO. **1**	A4
			SCALE:1:10	SHEET 1 OF 1